Cancer Cell

Report

Mutant KRAS peptide targeted CAR-T cells engineered for cancer therapy

Graphical abstract

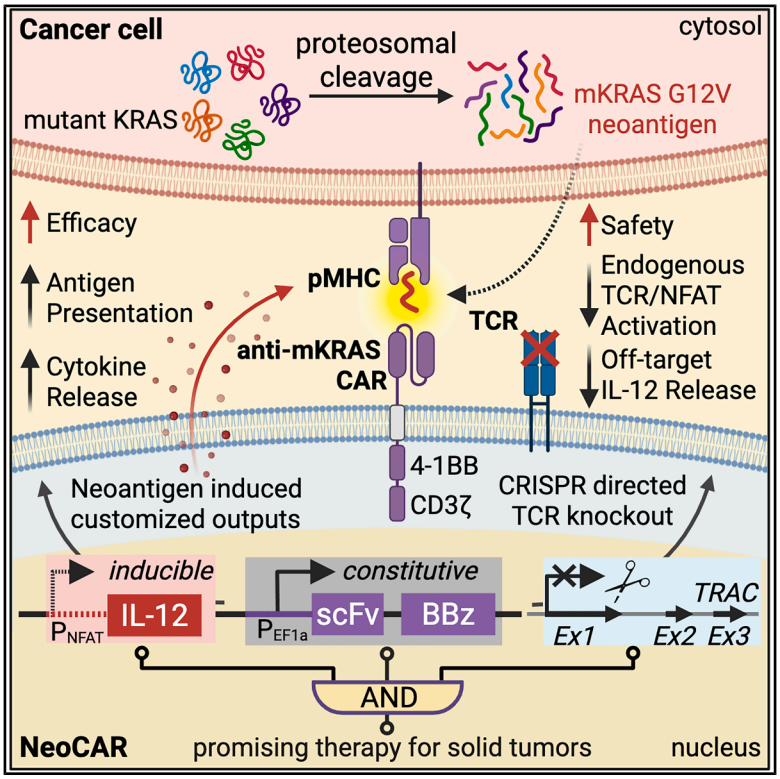

Highlights

- Engineered scFvs target mutant KRAS with high affinity and specificity *in vitro*
- Oncogenic KRAS directed NeoCARs exhibit anti-tumor response *in vitro* and *in vivo*
- NeoCARs armored with inducible IL-12 upregulate antigen availability and enhance killing
- TCR knockout improves the safety of iIL-12 NeoCARs *in vivo*

Authors

Alexander Benton, Jiageng Liu, Mathilde A. Poussin, ..., Matthew D. Beasley, Ben R. Kiefel, Daniel J. Powell, Jr.

Correspondence

poda@pennmedicine.upenn.edu

In brief

Benton et al. identify binders against common mutant KRAS neoantigens and create peptide-centric CAR-T cells (NeoCARs). NeoCARs demonstrate a robust anti-tumor response against cancer cells expressing mutant KRAS peptides by MHC, both *in vitro* and *in vivo*. Inducible cytokine release and TCR deletion further enhance the therapeutic index.

Benton et al., 2025, Cancer Cell *43*, 1–12
July 14, 2025
https://doi.org/10.1016/j.ccell.2025.05.006

CellPress

Cancer Cell

CellPress

Report

Mutant KRAS peptide targeted CAR-T cells engineered for cancer therapy

Alexander Benton,[1,2,8] Jiageng Liu,[1,7,8] Mathilde A. Poussin,[1] Andrea Lang Goldgewicht,[1] Madhara Udawela,[3] Adham S. Bear,[1,4] Nils Wellhausen,[1,4] Beatriz M. Carreno,[1,5,6] Pete M. Smith,[3] Matthew D. Beasley,[3] Ben R. Kiefel,[3] and Daniel J. Powell, Jr.[1,5,6,9,*]

[1]Center for Cellular Immunotherapies, Perelman School of Medicine at the University of Pennsylvania, Philadelphia, PA 19104, USA
[2]Pharmacology Graduate Group, Perelman School of Medicine, University of Pennsylvania, Philadelphia, PA 19104, USA
[3]Myrio Tx, Melbourne, VIC, Australia
[4]Division of Hematology-Oncology, Department of Medicine, Perelman School of Medicine, Philadelphia, PA 19104, USA
[5]Parker Institute for Cancer Immunotherapy, Perelman School of Medicine at the University of Pennsylvania, Philadelphia, PA 19104, USA
[6]Department of Pathology and Laboratory Medicine, Perelman School of Medicine at the University of Pennsylvania, Philadelphia, PA 19104, USA
[7]Bioengineering Graduate Group, Department of Bioengineering, University of Pennsylvania, Philadelphia, PA 19104, USA
[8]These authors contributed equally
[9]Lead contact
*Correspondence: poda@pennmedicine.upenn.edu
https://doi.org/10.1016/j.ccell.2025.05.006

SUMMARY

Despite the success of chimeric antigen receptor (CAR)-T cell therapies in hematological malignancies, clinical success against solid tumors is limited due to low therapeutic efficacy or dose-limiting toxicity. Developing therapies that trigger potent, yet manageable, immune responses capable of eliminating highly heterogeneous and immunosuppressive tumor cell populations remains a key challenge. Here, we harness multiple genetic approaches to develop a CAR-T cell therapy targeting tumors. First, we screen binders targeting oncogenic KRAS G12V mutations presented by peptide-MHC complexes. Subsequently, we incorporate these neoantigen binders into CAR-T cells (mKRAS NeoCARs) and demonstrate their efficacy in xenograft models of metastatic lung, pancreatic, and renal cell cancer. Finally, we enhance the *in vivo* efficacy and safety profile of mKRAS NeoCARs via inducible secretion of IL-12 and T cell receptor deletion. Together, these screening and engineering processes provide a modular platform for expanding the therapeutic index of cellular immunotherapies that target cancer.

INTRODUCTION

Engineered T cell immunotherapies have successfully treated hematological malignancies.[1–4] However, adaptations of these therapies for the treatment of solid tumors have met significant roadblocks. Therapeutic failure is common due to increased tumor burden,[5] or the lack of immune cell trafficking into an immunosuppressive tumor microenvironment.[6,7] In cases where clinical activity has been observed, unregulated T cell activation[8,9] or on-target/off-tumor antigen recognition[10,11] has resulted in life-threatening toxicities, indicating a significantly smaller therapeutic window for cellular immunotherapies in solid tumors.

The limited presence of homogenously expressed tumor-specific surface antigens has hindered the treatment of solid tumors,[12] resulting in antigen negative relapse[13] and cytotoxicity in healthy tissue.[10,11] Oncogenic driver mutations are theoretically ideal targets for cell therapies. However, most of these candidates are intracellular proteins that are only visible on the cell surface as peptide-MHC (pMHC) neoantigens,[14] limiting their accessibility to conventional CARs. While tumor infiltrating lymphocytes[15] (TILs) commonly recognize neoantigens, a small subset of neo-epitopes elicit immunogenicity by endogenous T cell receptors[16] (TCRs), and fewer are publicly shared by large patient populations.[17]

One exception is mutant KRAS (mKRAS) which is present in ~20% of all solid tumors with >75% of activating mutations occurring at codon G12.[18] Processing and presentation of KRAS G12X mutations in the most globally prevalent HLA types[19] indicates that mKRAS neoantigen targeted therapies could be utilized in large patient populations if binders with sufficient affinity and specificity are developed. We and others have previously identified TCRs targeting HLA class I-restricted mKRAS, demonstrating robust anti-tumor responses.[20,21] However, analogous CAR-based approaches with high-affinity binders have yet to be developed. Unlike TCRs, CAR constructs incorporate co-stimulatory domains that enhance T cell activation and persistence, and may expand patient accessibility by facilitating the development of "off-the-shelf" products[22] through further genetic modifications, such as TCR knockout, which can be integrated in CAR products to prevent graft-versus-host disease

Please cite this article in press as: Benton et al., Mutant KRAS peptide targeted CAR-T cells engineered for cancer therapy, Cancer Cell (2025), https://doi.org/10.1016/j.ccell.2025.05.006

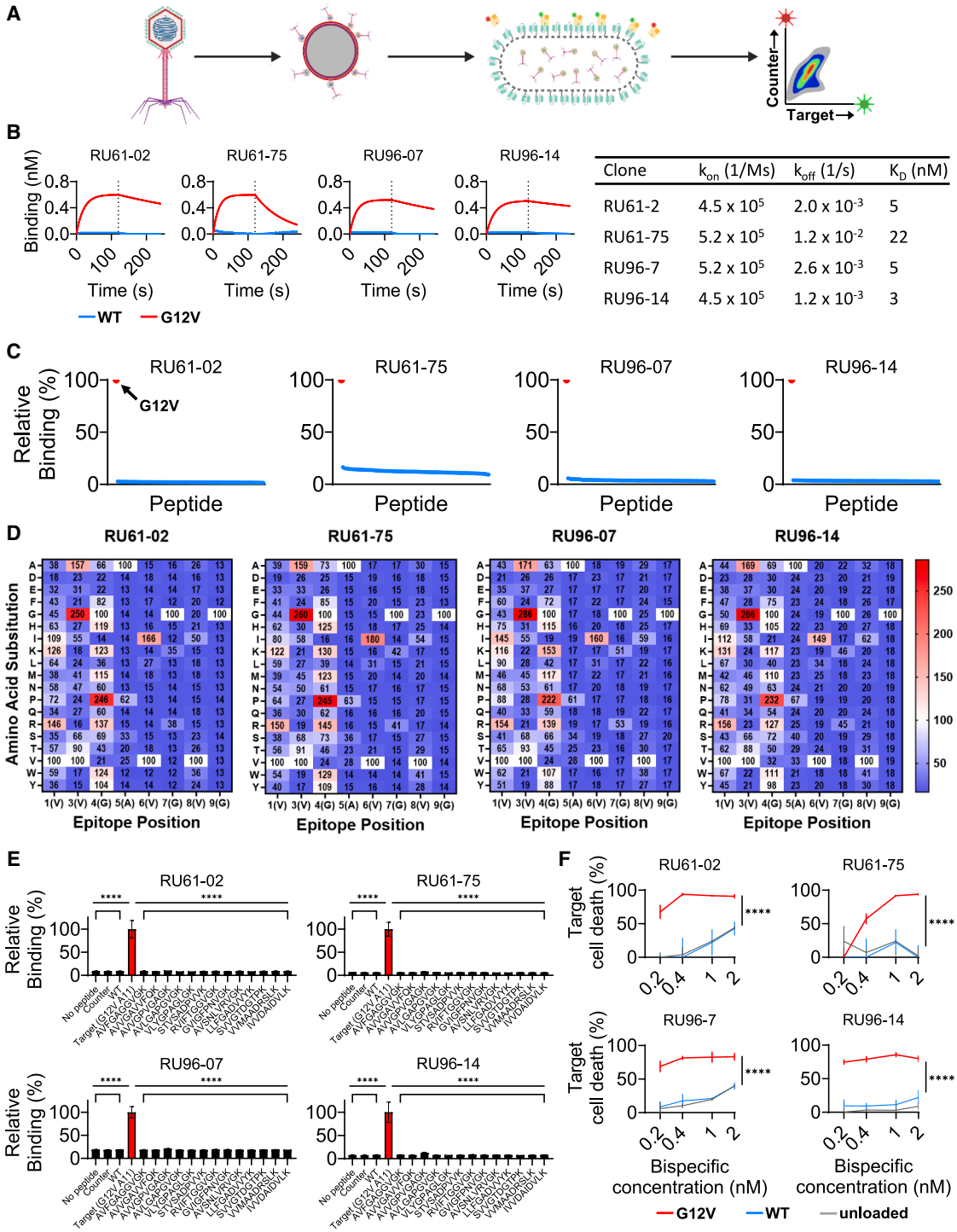

Figure 1. Isolation and characterization of anti-mKRAS pMHC scFvs

(A) The Retained Display (ReD) library comprises scFvs displayed on the capsid of a lambdoid phage. ScFvs were initially panned against magnetic beads coated with the pMHC of interest. The display modality was then transferred to the cell wall of a permeabilized bacterial cell. The target pMHC was labeled with one fluorophore (shown here in green) while counter-target pMHCs were labeled with a different fluorophore (shown in red). Labeled permeabilized cells were then sorted for clean target binding by FACS to identify scFvs.

(B) Kinetic traces of anti-mKRAS G12V A*11:01 binders against both G12V and WT complex. G12V or WT KRAS pMHC were associated with probe-loaded biotinylated scFv. Measurement of association/dissociation was measured by BLI.

(legend continued on next page)

Please cite this article in press as: Benton et al., Mutant KRAS peptide targeted CAR-T cells engineered for cancer therapy, Cancer Cell (2025), https://doi.org/10.1016/j.ccell.2025.05.006

(GvHD).[23] Nonetheless, the low abundance of some neoantigens on the tumor cell surface may still limit the efficacy of CAR and TCR based therapies.[21,24] Thus, it may be essential to concurrently develop specific binders and increase T cell potency to achieve clinically effective NeoCAR therapy.

Endowing T cell therapies with secondary genetic modifications is a promising method for enhancing therapeutic efficacy.[22,25] Ectopic expression of soluble immune modulators such as IL-2,[26] IL-12,[27] and IL-18[28] have shown significant improvements in tumor control, but may also result in dose limiting toxicities,[9,29] emphasizing the need for these molecules to work within a tight therapeutic window. Recently, our group achieved this goal using a single vector platform, UniVect, to program CAR-T cells with inducible transgene expression, including IL-12, upon antigen recognition.[30] We have shown that inducible IL-12 (iIL-12) amplifies IFN-γ secretion by engineered T cells that may secondarily upregulate MHC-1 mediated antigen presentation by tumor cells to amplify anti-tumor efficacy. The iIL-12 significantly improved the CAR-T safety profile over constitutive systems with remaining toxicity concerns. A possible mechanism of toxicity in CAR T cells expressing iIL-12 is a positive feedback loop between endogenous TCR-sensitivity and IL-12 expression, regulated by nuclear factor of activated T cells (NFAT) in the UniVect platform. Therefore, endogenous TCR ablation could expand the safety profile of NFAT promoter-driven IL-12 expression systems preventing responses to unintended targets.

In this report, we demonstrate techniques for expanding the therapeutic window of CAR-T cells targeting human tumors using single-chain variable fragments (scFvs) specific to the KRAS G12V epitope presented by pMHC (NeoCARs). Next, we increase preclinical activity through armoring NeoCARs with NFAT inducible IL-12 production using the UniVect platform. Finally, we incorporate TCR knockout to eliminate dysregulated T cell activity and demonstrate an expanded therapeutic window in an established preclinical xenograft model of non-small cell lung cancer (NSCLC).

RESULTS

Isolation and characterization of anti-KRAS G12V neoantigen human single chain antibodies

Antibodies specific to the KRAS G12V epitope (residues 7–16) in complex with recombinant human HLA-A*11:01 protein were obtained from the Retained Display (ReD) scFv library, which contains >10^{11} pairings of human germline V_H and V_L that are productively folded in the *Escherichia coli* cytoplasm[31] (Figure 1A). ReD allows the retention and intracellular display of exogenous targets within detergent-permeabilized bacteria to the binding antibodies, therefore avoiding the need for the antibody transport to the cell surface. This powerful platform significantly improves the screening efficiency for human scFv frameworks and has been used to develop peptide-centric CARs for neuroblastoma.[32] We employed this system to identify KRAS G12V binders with high affinity. Four clones were isolated that differentially bound the KRAS G12V (7–16) A*11:01 complex but not wild-type (WT) KRAS pMHC, with K_D values ranging from 3 to 22 nM (Figure 1B).

Initial screening of each clone confirmed an absence of binding to 96 unrelated HLA-A*11:01 pMHC complexes that are known to be presented *in vivo,*[33] indicating that the interaction with the KRAS G12V complex was specific and contextual (Figure 1C). To obtain an inferred interaction map between the scFvs with the KRAS G12V A*11:01 epitope side chains, peptides with substitutions of each non-anchor position of the KRAS G12V peptide with each amino acid, except cysteine, were refolded as A*11:01 pMHC complexes (Figure 1D). This X-scan analysis shows that all four clones had a similarly broad footprint, which extended over the last five residues of the peptide. There was a strong preference for the mKRAS neoantigen sequence identity at positions 5, 6, 7, 8, and 9, with position 9 showing complete intolerance for any substitution. Notably, the G12V neoantigen mutation site at position 6 of the peptide only tolerated a conservative isoleucine substitution. Positions 1, 3, and 4, although more permissive than the middle/C-terminal of the epitope, did still show a preference for the neoantigen identity, although position 3 was notable for a preferred exchange of the valine to smaller side chains of alanine and glycine, suggesting a steric hindrance for scFv binding at that position.

The X-scan enabled a predicted pMHC binding motif for the scFv clones to be assessed for off-target binding to peptides known to be presented by the normal tissue immunopeptidome using algorithms sCRAP[32] and eXpitope 2.0.[34] All scFv clones showed specific binding only to the KRAS G12V (7–16) A*11:01 complex, and not to any of the top 14 peptides identified by the algorithms (Figure 1E).

To demonstrate the capability of the clones to direct specific $CD8^+$ T cell killing, they were expressed as tandem scFv T cell engager (TCE) bispecifics through fusion to anti-CD3.[35] The target KRAS G12V peptide or KRAS wildtype peptide (7–16) was loaded onto HLA-A*11:01 expressing K562 target cells with empty MHC complexes. All four A*11:01 anti-pMHC clones displayed killing that was dependent on bispecific concentration and KRAS G12V peptide complex loading (Figure 1F). These data demonstrated that the clones generated were highly

(C) Specificity assays for all clones. 96 unrelated A*11:01 pMHC complexes from 10-mer peptides known to be presented by the immunopeptidome were tested for binding to clones, along with the target mKRAS G12V pMHC (red). Relative binding is shown as a percentage of mKRAS G12V binding.
(D) X-scan analysis. Each position of the mKRAS G12V (7–16) epitope, aside from the anchor residues the second and terminal positions, were substituted for every amino acid other than cysteine and refolded as pMHC. Binding by scFvs was assessed as a percentage relative to the mKRAS G12V 10-mer pMHC complex.
(E) Sequence-related off-target binding by the mKRAS binders. Sequences with homology to the KRAS peptide that are known to be presented by the immunopeptidome were refolded as pMHC and assessed for binding to RU96-14. Relative binding is shown as a percentage of mKRAS G12V binding ($n = 2$) (ordinary ANNOVA). ****; $p < 0.0001$.
(F) *In vitro* T cell engager (TCE) bispecific killing. K562 cells expressing HLA-A*11:01 were loaded with exogenous mKRAS peptide or WT peptide at 1 μM. Tandem scFv TCE bispecific was titrated against target cell killing ($n = 3$) (2-way ANNOVA vs. KRAS G12V). ****; $p < 0.0001$. All data with error bars are presented as mean ± SD. All data are representative of two or more experiments.

Please cite this article in press as: Benton et al., Mutant KRAS peptide targeted CAR-T cells engineered for cancer therapy, Cancer Cell (2025), https://doi.org/10.1016/j.ccell.2025.05.006

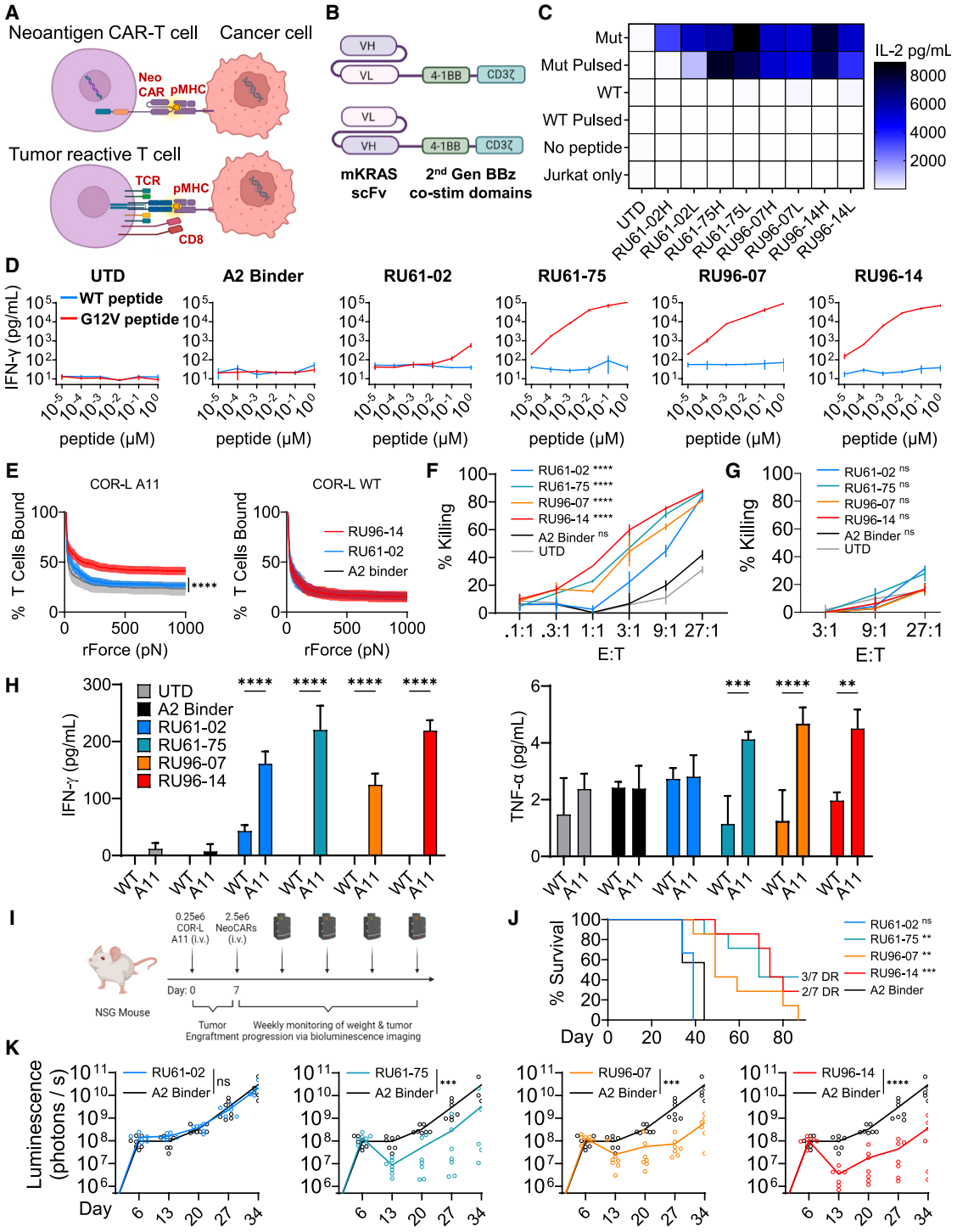

Figure 2. Design and validation of mKRAS NeoCARs targeting G12V presented by HLA A*11:01

(A) Schematic comparison of a NeoCAR and a tumor reactive T cells.

(B) Second generation Neoantigen CARs with 4-1BB and CD3ζ costimulatory domains were generated with alternate orientations preceded by the variable heavy (VH) or light (VL) chain.

(C) IL-2 secretion by Jurkat cells transduced with lentiviral vectors containing the indicated CAR, co-cultured with the peptide loaded target cells for 24h ($n = 3$). K562 cells expressing HLA A*11:01 were incubated in 1uM mutant (VVVGAVGVGK) or WT (VVVGAGGVGK) peptides for 90 min. Media was refreshed for the pulsed conditions.

(legend continued on next page)

Please cite this article in press as: Benton et al., Mutant KRAS peptide targeted CAR-T cells engineered for cancer therapy, Cancer Cell (2025), https://doi.org/10.1016/j.ccell.2025.05.006

specific for the KRAS G12V (7–16) A*11:01 complex and could redirect potent anti-tumor activity by T cells.

Screening and validation of mKRAS NeoCARs

As a route toward therapeutic enhancement, candidate mKRAS binders were incorporated into NeoCAR-T cells capable of recognizing target pMHC independent of canonical TCR and CD8 recognition (Figure 2A). Candidate scFvs were cloned into lentiviral transfer plasmids[36] encoding 2nd generation 4-1BB/CD3ζ CARs in alternate heavy and light (V_H and V_L) orientations (Figure 2B). To screen for CAR activity, Jurkat cells were transduced with the candidate NeoCARs and co-cultured with A*11:01 expressing target cells, either continuously loaded or transiently pulsed with KRAS peptide epitopes for 90 min to simulate varying levels of antigen presentation and examine how transient versus sustained antigen availability impacts NeoCAR responses. All NeoCARs, except RU61-02, responded specifically to mutant peptides with no consistent association between V_H/V_L orientation and CAR stimulation (Figure 2C). Therefore, the four binders in their initially developed V_L-V_H orientation were selected for further preclinical development.

Because KRAS neoantigens are often presented at <100 copies per cell,[21] we assessed the dependence of mKRAS NeoCAR on antigen density to elicit an anti-tumor response. The four candidate CARs and a separately developed and unmatched KRAS G12V A*02:01 control CAR (A2 Binder) were transduced into primary human T cells. Three of four candidates produced higher levels of IFN-γ in response to titered mKRAS peptide (Figure 2D). NeoCAR RU61-02 had a weaker response to the target neoantigen and produced basal amounts of IFN-γ at mKRAS concentrations where the other candidates exhibited maximal output. Similarly, NeoCAR RU61-02 secreted little IL-2 against pulsed target peptides compared to the other candidates (Figure 2C). To determine if this observation was related to affinity, NeoCARs were stained with an A*11:01 G12V pMHC Dextramer, effectively mimicking the target neoantigen[37] (Figure S1A). These Dextramers specifically bound CARs targeting A*11:01 G12V and at a roughly equivalent percentage to CAR transduction for the three lead candidates. NeoCAR RU61-02 stained at a lower ratio of CAR to Dextramer, indicating a weaker scFv-target interaction. Co-staining with anti-CD8 confirmed CD8 independent neoantigen binding (Figure S1B). Differences in avidity were confirmed on a z-Movi device using monolayers of the NSCLC cell line COR-L23 that harbors an endogenous KRAS G12V mutation, transduced with HLA A*11:01 (COR-L A11)[21] (Figure 2E).

Anti-tumor activity *in vitro* was tested initially against COR-L A11 cells expressing mKRAS G12V epitopes at endogenous levels. We observed similar lysis by the three lead candidates across a broad range of effector to target (E:T) ratios and lesser but still significant lysis by NeoCAR RU61-02 (Figure 2F). Higher E:T ratios (>1:1) were needed to achieve >50% killing, at which point bystander killing was observed, suggesting that neoantigen abundance limits NeoCAR activity. No specific lysis by NeoCARs was observed against WT control COR-L23 (COR-L WT) cells (Figure 2G). At a 3:1 E:T ratio, we observed IFN-γ and TNF-α secretion that was elevated against COR-L A11 cells, which was low compared to the maximum IFN-γ after peptide stimulation (Figures 2D and 2H). We next incorporated additional cell lines with an HLA-A*11:01 and KRAS G12V background to test specific lysis. CAKi-2, PANC-1, and HCC-827 cells, which endogenously express HLA-A11:01, were modified to harbor KRAS mutations, including G12V, using a tandem minigene construct (TMC). Conversely, YAPC, COR-L23, and SW-620 cells, which naturally express KRAS G12V, were transduced with an HLA-A11:01 plasmid. As a control, we included parental and HLA-A11:01-engineered BxPC-3 cells expressing wild-type KRAS. Surface expression of HLA-A*11:01 was confirmed in all cell lines, and KRAS-positive populations were isolated from CAKi-2, PANC-1, and HCC-827 parental lines (Figure S1D). Significant lysis was only observed in cell lines that co-express HLA-A11:01 and KRAS G12V, confirming the specificity of NeoCARs *in vitro* (Figure S2A).

To determine the preclinical efficacy of mKRAS NeoCARs *in vivo,* COR-L A11 cells expressing luciferase were used in an intravenous (i.v.) NOD/scid/γcnull (NSG) mouse model (Figures 2I and S1C–S1E). After confirming tumor engraftment by bioluminescence imaging (BLI), mice received 2.5e6 mKRAS NeoCAR T cells. All three lead candidates mediated initial reductions in tumor burden and improved survival, with RU61-75 and RU96-14 NeoCARs producing a subset of durable responses (2/7 and 3/7 respectively) defined by lower tumor burden at the conclusion of the experiment than at CAR-T dosing (Figure 2J and 2K). Significant tumor reduction over the control CAR was observed for three candidates (Figures 2K and S2B) yet tumor relapse was observed in most mice. The remaining mice in the NeoCAR-treated cohort showed sustained tumor burden reduction with no evidence of toxicity through day 90, with regular clinical monitoring including signs of poor grooming, hunched posture, labored breathing, excessive weight loss, and other indicators of distress. We then incorporated additional tumor models with CAKi-2-G12V and YAPC-A11 delivering metastatic renal and pulmonary carcinoma respectively. In both models, we

(D) IFN-γ secretion by primary NeoCARs after 24h of co-culture with K562 cells expressing HLA A*11:01 and titered additions of mutant or WT peptides ($n = 3$).
(E) Z-Movi avidity data for high affinity (RU96-14), low affinity (RU61-02), and non-targeting NeoCARs on a monolayer of COR-L A11 targets cells or COR-L WT control cells ($n = 4$) (ordinary ANOVA).
(F) Lysis of the G12V mutant cell line COR-L23 transduced with HLA A*11:01/GFP/Luciferase (COR-L A11) by NeoCARs. A NeoCAR binding HLA A*02:01 (see Figure S2) was used as a non-targeting control ($n = 4$) (two-way ANOVA vs. UTD).
(G) Lysis of COR-L WT control cells transduced with GFP/Luciferase by NeoCARs ($n = 4$) (two-way ANOVA vs. UTD).
(H) IFN-γ and TNF-α secretion at the 3:1 E:T from co-cultures in main Figure 2F ($n = 4$) (two-way ANOVA).
(I) *In vivo* study design. CAR-T cells were injected i.v. at 2.5e6 CAR+ cells per mouse in NSG mice with established COR-L A11 tumors expressing ($n = 7$ mice per group).
(J) Percentage survival in each NeoCAR *in vivo* group (log rank Mantel-Cox test vs. A2 Binder).
(K) Quantified tumor luciferase activity (two-way ANOVA of NeoCARs vs. A2 binder). NS; not significant, **; $p < 0.01$, ***; $p < 0.001$, ****; $p < 0.0001$. All data with error bars are presented as mean ± SD. All data are representative of two or more experiments. See also Figures S1, S2 and Table S1.

Please cite this article in press as: Benton et al., Mutant KRAS peptide targeted CAR-T cells engineered for cancer therapy, Cancer Cell (2025), https://doi.org/10.1016/j.ccell.2025.05.006

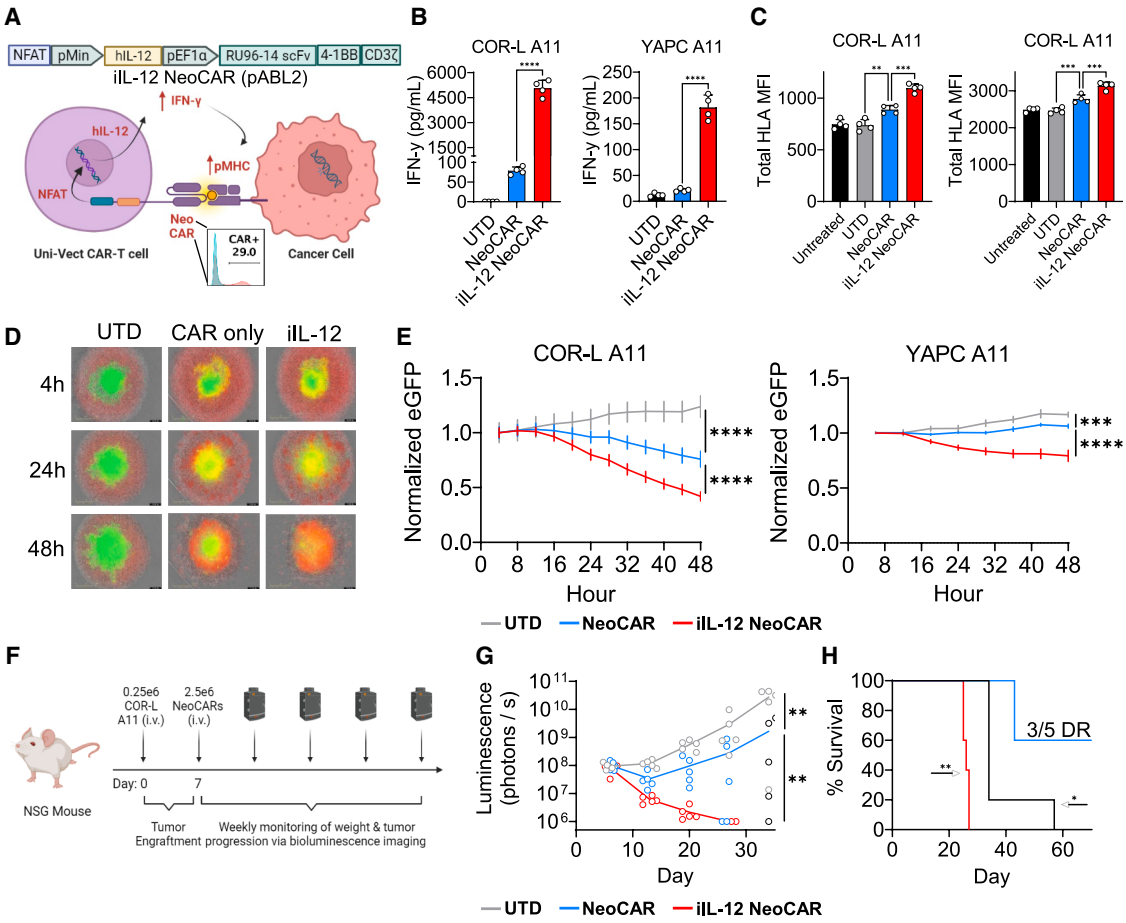

Figure 3. Inducible IL-12 enhances anti-tumor activity of mKRAS NeoCARs

(A) The iIL-12 UniVect construct with a mKRAS NeoCAR and schematic showing a modified activation pathway after lentivirus transduction. Histogram of primary T cells transduced and stained with α-human Fc.

(B) IFN-γ secretion by iIL-12 armored NeoCARs after 24h co-culture with COR-L A11 and YAPC A11 target cell lines ($n = 4$) (Student's t test).

(C) Supernatants from (B) were added to freshly plated tumor cells. Total HLA expression was measured by flow cytometry after 24h ($n = 4$) (Student's t test).

(D) Representative confocal microscopy showing co-culture of COR-L A11 spheroids (green) and T cells (red).

(E) Killing of COR-L A11 (left) and YAPC A11 (Right) target cell spheroids by iIL-12 NeoCARs over 48h ($n = 4$) (two-way ANOVA vs. NeoCAR).

(F) *In vivo* study design. CAR-T cells were injected i.v. at 2.5e6 CAR+ cells per mouse in NSG mice with established COR-L A11 tumors expressing ($n = 5$ mice per group).

(G) Quantified tumor luciferase activity (two-way ANOVA iIL-12 NeoCAR vs. NeoCAR).

(H) Percentage survival in each *in vivo* group (log rank Mantel-Cox test iIL-12 NeoCAR vs. NeoCAR). MFI; mean fluorescent intensity. *; $p < 0.05$, **; $p < 0.01$, ***; $p < 0.001$, ****; $p < 0.0001$. All data with error bars are presented as mean ± SD. All data are representative of two or more experiments. See also Figure S3 and Table S1.

observed an improved survival benefit with NeoCARs versus the A2 binder control as well as a significant tumor burden reduction (Figures S2C–S2E). However, the potency of NeoCARs required improvement to achieve complete tumor clearance, indicating additional genetic modifications of T cells might be required.

Enhancement of mKRAS NeoCARs with NFAT inducible IL-12

To enhance the therapeutic efficacy of mKRAS NeoCARs, we incorporated the pleiotropic cytokine IL-12. Due to toxicities associated with direct administration[38] and cellular therapy,[8] we utilized the UniVect platform that combines constitutive CAR and NFAT driven expression in a single vector to improve the safety profile of armored CAR-T cells.[30] NeoCAR RU96-14 was selected as the top candidate for further optimization and construct pABL2 was generated (Figure 3A top). IL-12 was selected for its known enhancement of IFN-γ responses.[39] We hypothesized that, upon mKRAS NeoCAR activation, induced IL-12 production would lead to upregulation of IFN-γ secretion by NeoCAR cells, and in turn, increased MHC-I antigen presentation on target cells[40–42] (including the G12V target), and thus enhanced tumor cell killing (Figure 3A, bottom).

Tight regulation of inducible (i)IL-12 production was confirmed after stimulation with mutant and WT peptide (Figure S3A). IL-12 output in the single pg/mL range increased the maximal output as well as the sensitivity of IFN-γ response in mKRAS NeoCARs (Figure S3B, left) compared to the NeoCAR alone (Figure S3B, right). When testing the IFN-γ response against endogenous

Please cite this article in press as: Benton et al., Mutant KRAS peptide targeted CAR-T cells engineered for cancer therapy, Cancer Cell (2025), https://doi.org/10.1016/j.ccell.2025.05.006

levels of G12V neoantigen in COR-L23 (NSCLC) and YAPC (pancreatic carcinoma) A*11:01 transduced cell lines,[21] a 1–2 log increase by the iIL-12 NeoCAR was observed (Figure 3B). IFN-γ secretion was also elevated by basal iIL-12, although at substantially lower levels, in the presence of WT HLA control cells (Figure S3C). Supernatants from the NeoCAR co-cultures containing elevated IFN-γ induced an increase in total HLA expression on freshly plated tumor cells and was increased further by supernatants from iIL-12 NeoCARs (Figure 3C). This increase was also observed to a lesser extent in WT control cell lines (Figure S3D). Interestingly, artificially expressed A*11:01 was upregulated similarly to endogenous HLA, indicating that expression is likely controlled at a post-translational level in this context[43] (Figure S3E).

To test for enhanced *in vitro* anti-tumor activity, iIL-12 NeoCARs were co-cultured with COR-L23 and YAPC spheroids. Fluorescence microscopy showed increased CAR-T cell infiltration and killing of target COR-L A11 spheroids over a 48h period (Figure 3D) leading to higher levels of killing of both target cell lines due to iIL-12 (Figure 3E), which was not observed against WT controls (Figure S3F). Together, these data support the hypothesis that iIL-12 increases mKRAS NeoCAR target killing and can overcome the challenge of low neoantigen abundance.

To assess the therapeutic index of iIL-12 mKRAS NeoCARs, *in vivo* studies were conducted at two different CAR-T cell doses. First, mice received the same CAR-T cell doses of 2.5e6 (Figure 3F) as in the initial NeoCAR characterization experiment (Figure 2I). Consistent with our *in vitro* data, rapid tumor clearance was observed in mice receiving iIL-12 NeoCARs, compared to a lesser, but significant, response in mice receiving the NeoCAR alone (Figure 3G). However, all mice receiving iIL-12 NeoCARs required sacrificing due to severe toxicity approximately two weeks after treatment. As a result, there was a decreased survival benefit compared to the NeoCAR alone group, in which 3/5 mice survived the duration of the experiment (Figures 3H and S3G). Given the increase in initial tumor clearance by iIL-12 NeoCARs, we repeated the *in vivo* study at a lower dose (0.8e6 CAR-T cells/mouse) to detect a potential shift in the therapeutic window (Figure S3H). Modest, but insignificant, improvements in tumor control (Figures S3I and S3J) and survival (Figure S3K) were observed in mice treated with iIL-12 NeoCARs, with no benefit from the CAR alone. These experiments demonstrate the potential of iIL-12 to enhance the efficacy of mKRAS NeoCARs but simultaneously introduce a set of safety concerns that are common to solid tumor therapies. For clinical translation to be feasible, further improvements to the safety profile would be necessary.

TCR knockout to eliminate risks of systemic toxicity while preserving Neo-CAR activity

We previously described toxicity caused by ectopic IL-12 production by T cells in NSG mouse models, albeit in a constitutive expression system.[30] We also showed both CAR and endogenous TCR mediated activation leads to NFAT inducible expression, and that knockout (KO) of the TCR rendered CARs the exclusive antigen-mediated activators. Given past instances of iIL-12 toxicity in cell therapy,[8] we posited that unregulated IL-12 expression via TCR mediated xenoreactivity caused the toxicity observed in mice treated with iIL-12 NeoCARs. We hypothesized that TCR KO would eliminate this toxicity and enable the safe administration of iIL-12 mKRAS NeoCARs.

We generated T cell products to compare the effects of the NeoCAR, iIL-12, and TCR KO (Figure 4A). Following CRISPR/Cas9-mediated TCR KO, enrichment of TCR-cells, and expansion, the KO groups were ∼99% TCR negative (Figure S4A). *In vitro* stimulation demonstrated NFAT inducible production of IL-12 by transduced products in response to cell stimulation cocktail (CSC), through their TCRs (via anti-CD3), or their CARs (via COR-L A11 target cells) (Figure S4B). Measurement of the resulting IFN-γ response (Figure 4B) showed log-fold increases in production by anti-CD3 activated cells producing iIL-12 that was reduced over 97% by TCR KO. This remnant activity in the KO population is consistent with the small number of TCR-positive cells remaining after enrichment. The IFN-γ response to target cells was nearly 2-log greater in iIL-12 NeoCARs than NeoCARs alone, and TCR KO did not reduce output. Interestingly, the iIL-12 only T cells produced a greater amount of IFN-γ than the NeoCAR alone against COR-L A11. A similar amount of activity was observed in co-cultures of WT COR-Lcells with both TCR-expressing iIL-12 T cell groups, which indicated low level TCR-mediated allo-recognition. Spheroid assays showed that iIL-12 led to increased killing regardless of the presence of the target neoantigen (Figure S4C). However, against both target and non-target cells, TCR KO eliminated alloreactivity while maintaining cancer cell killing via the NeoCAR, supporting the notion that iIL-12 exacerbates low level TCR-mediated xeno- or alloreactivity, and that TCR KO restores safety.

To determine if the coalesce of NeoCAR, iIL-12, and TCR KO expands the therapeutic index, we conducted an *in vivo* experiment using the same 2.5e6 CAR-T dose that led to lethal toxicity in iIL-12 NeoCARs and limited efficacy with the NeoCAR alone (Figure 4C). Once again, we saw rapid tumor clearance by iIL-12 NeoCARs that was greater than with NeoCAR alone (Figure 4D). Importantly, TCR KO did not impair anti-tumor activity. A delayed reduction in tumor burden was observed in animals that received iIL-12 only T cells, which corresponded with weight loss in TCR+ iIL-12 and iIL-12/NeoCAR groups (Figures S4D and S4E). These animals were euthanized due to severe toxicity, reinforcing the notion that the combination of iIL-12 and TCR activation is detrimental to the safety profile of mKRAS NeoCARs. iIL-12 TCR-mediated toxicity resulted in reduced survival benefit compared to the NeoCAR alone group, and survival benefit was improved further when TCR KO was incorporated into iIL-12 NeoCAR therapy (Figure 4E). Notably, all animals that received iIL-12 NeoCARs with TCR KO achieved complete response and survived the duration of the experiment without evidence of tumor progression or toxicity (Figures 4D and 4E).

Peripheral blood sampling captured the mechanism of xenoreactivity in TCR+ iIL-12 groups. At day 18, tumors had cleared in the iIL-12 NeoCAR groups and were decreasing in the iIL-12 only group, with circulating human T cells detectable in all mice. On day 25, when toxicity was mounting in TCR+ iIL-12 T cell groups, human T cell counts increased (Figure 4F) in TCR+ iIL-12 and TCR+ iIL-12 NeoCAR T cell groups, as did serum IL-12 (Figure 4G) and IFN-γ (Figure 4H). In the TCR KO iIL-12 NeoCAR and TCR+ NeoCAR groups, all three of these readouts decreased between days 18 and 25. Thus, TCR signaling and iIL-12 combine to cause a sustained immune reaction that is detrimental

Please cite this article in press as: Benton et al., Mutant KRAS peptide targeted CAR-T cells engineered for cancer therapy, Cancer Cell (2025), https://doi.org/10.1016/j.ccell.2025.05.006

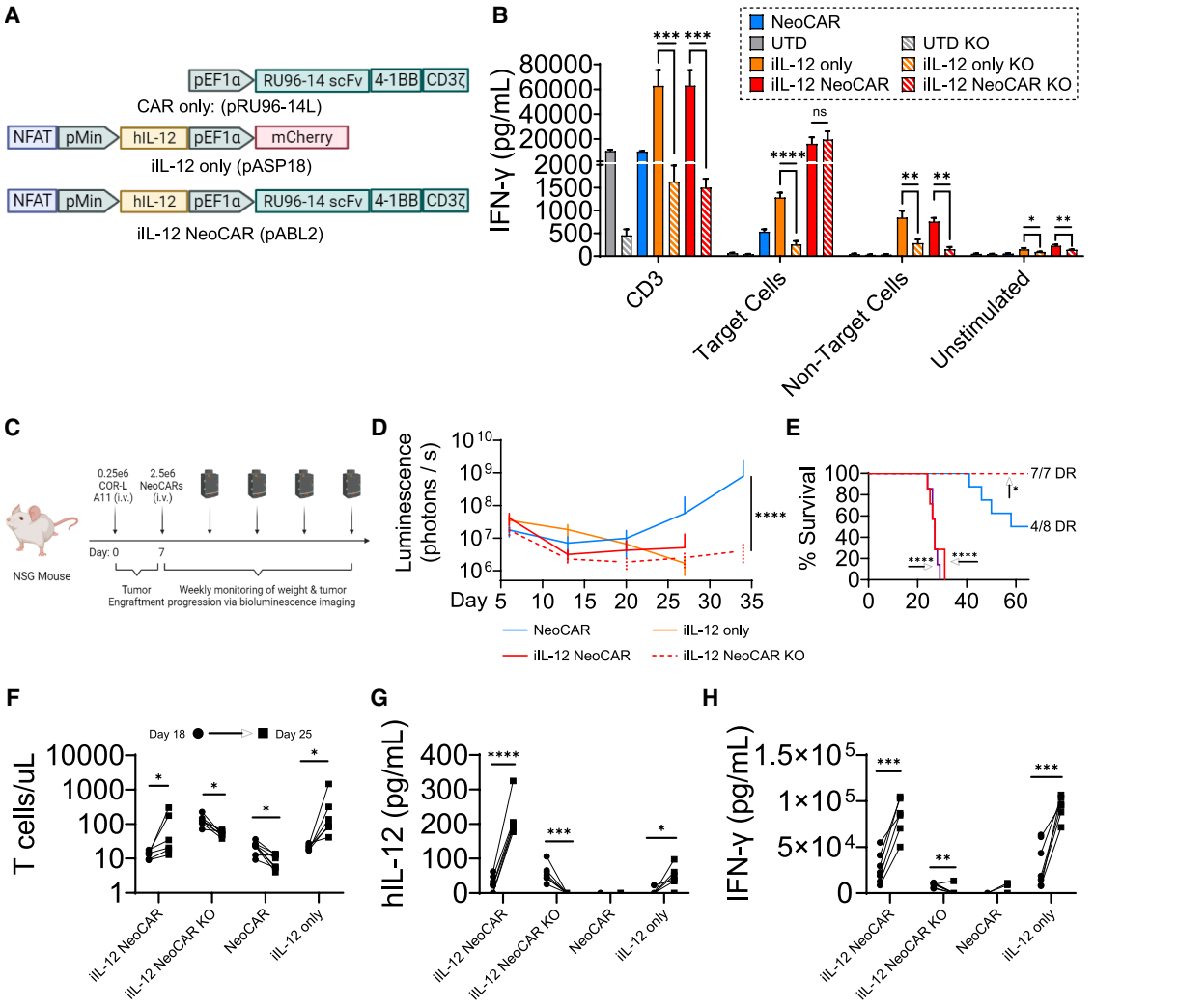

Figure 4. TCR Knockout expands therapeutic window of iIL-12 NeoCARs

(A) Schematic representation of compared constructs/experimental groups.

(B) IFN-γ secretion induced by 24 h stimulation with plate bound anti-CD3, target COR-L A11, or control CORL WT cells in TCR+ and TCR knockout T cells ($n = 4$) (Student's *t* tests).

(C) *In vivo* study design. CAR-T cells were injected i.v. at 2.5e6 CAR+ cells per mouse in NSG mice with established COR-L A11 tumors expressing (n = 7–8 mice per group).

(D) Quantified tumor luciferase activity compared (two-way ANOVA of iIL-12 NeoCAR TCR KO vs. NeoCAR).

(E) Percentage survival in each *in vivo* group (log rank Mantel-Cox test of iIL-12 NeoCAR TCR KO vs. NeoCAR).

(F) CD4/8 + T cell counts in peripheral blood at day 18 and day 25 (paired T tests).

(G) Serum levels of hIL-12 at day 18 and day 25 (paired T tests).

(H) Serum levels of IFN-γ at day 18 and day 25 (paired T tests). ns; not significant, *; $p < 0.05$, **; $p < 0.01$, ***; $p < 0.001$, ****; $p < 0.0001$. All data with error bars are presented as mean ± SD. All data are representative of two or more experiments. See also Figure S4 and Table S1.

to the safety of the therapy, and removing the endogenous TCR as a source of unintended activation expands the therapeutic index of mKRAS NeoCARs.

DISCUSSION

Prior reports demonstrate that TCRs are naturally obtainable for immunotherapy development, including against KRAS G12V epitope,[21,44] but engineering CAR-T therapies in the same target class requires the generation of TCR mimics. The paucity of reports of CARs successfully targeting pMHC has been due in part to difficulties in obtaining antibodies that are specific to a single peptide-MHC,[45] including mKRAS,[46] where the lack of sensitivity and selectivity resulted in an inability to specifically recognize endogenous mKRAS and HLA-A11 *in vitro*. In contrast, the ReD identified anti-pMHC antibodies against the KRAS G12V neoantigen. These antibodies displayed a broad footprint on the mKRAS epitope giving the binding a contextuality and selectivity required for specific targeting of native mKRAS pMHC by T cells via CARs.

Please cite this article in press as: Benton et al., Mutant KRAS peptide targeted CAR-T cells engineered for cancer therapy, Cancer Cell (2025), https://doi.org/10.1016/j.ccell.2025.05.006

Nonetheless, mKRAS neoantigen levels have been quantitated at fewer than 100 copies presented per cell,[21] which is several orders of magnitude lower than traditional CAR-T targets, akin to instances of antigen escape from the tumor cell surface.[24,47] Although we demonstrated T cell responsiveness at low antigen levels *ex vivo*, the NeoCARs only achieved full tumor control in a subset of animals *in vivo* (Figures 2I–2K). This partial *in vivo* control may result in part from an inability of the CAR to detect and signal an engagement with a low-abundance pMHC complex (sensitivity), or the inability to convert binding events into an immune synapse that kills the target cancer cell (potency).

IL-12 has garnered significant attention in the field of cellular immunotherapy, leading to several clinical trials.[48] Known for its role in autoimmunity[49] and immune-related complications in response to infection,[50] IL-12 has been associated with toxicity due to unregulated T cell responses. We utilized UniVect[30] to better regulate the immune response in NeoCARs, leading to increased activation-dependent secretion of IFN-γ which resulted in increased surface expression of HLA molecules, sensitizing cancer cells to immune recognition *in vitro*, however we still observed severe *in vivo* toxicity at doses required for tumor control (Figures 3F–3H). Our findings indicated that iIL-12 alone induced lethal toxicity in NSG mice when expressed by primary T cells (Figure 4E), which we postulated was due to TCR mediated xenoreactivity. In this line, combining iIL-12 NeoCAR with TCR KO resulted in robust tumor clearance and enhanced survival by preventing T cell xenoreactivity (Figure 4). Collectively, these genetic modifications expanded the therapeutic window and improved overall survival. It also suggests that alternative inducible payloads that augment HLA expression on cancer cells, such as IFN-γ itself, may improve peptide-specific CAR T cell activity. While IFN-γ is critical for CAR T cell-mediated myeloid activation and tumor killing, it lacks the broader immunomodulatory capabilities of IL-12. For instance, IL-12 enhances antigen presentation and innate immune responses more effectively than IFN-γ alone.[51]

This work exemplifies the extension of CAR-T cell therapies to pMHC epitopes. The prevailing view of the field is that second-generation CARs are limited to use for non-pMHC surface proteins that have 1,000s of copies per cell[52] and would lack the sensitivity of TCRs for deployment against pMHC species, which are typically <100 copies per cell. Attempts to engineer CARs for higher sensitivity and/or potency have included permuting the identity and number of cytoplasmic ITAM motifs,[53] or harnessing the known sensitivity of TCRs through fusing single-chain antibodies to integral chains of the TCR complex, either the α and β[54] or ε chain.[55] Our study shows that CARs can be effective *in vivo* against low abundance pMHC targets and enhanced through additional immune stimulation. NeoCAR activity against low abundance pMHC complexes might be attributed to the target class, as CARs using anti-pMHC scFvs have been shown to recapitulate a natural immune synapse,[56] in contrast to a non-canonical synapse for non-pMHC targets.[57]

Unlike TCRs, CARs offer the advantages of modular engineering to attenuate activity and a single ORF for integration. With a more streamlined manufacturing process, CAR-Ts may be produced more cost-efficiently and quickly without the needs to be personalized from each patient. Furthermore, our demonstration of potent, on-target killing in CAR-T cells with TCR KO and NFAT-inducible IL-12 predicts their use for allogeneic cellular immunotherapies, in either T or NK lineages that have been genome edited for these and further modifications, such as HLA deletion for immune tolerance.

As cellular immunotherapy progresses to include therapies for solid tumors, we anticipate the emergence of new generations of CAR-T cells with multiple genetic modifications as leading candidates. Where efficacy is achieved, there must also be consideration of the existence of a therapeutic window. We expect our approach to lay the groundwork for strategies that will usher in the future of safe and effective cellular therapies for solid tumors.

At present, our study is limited to a single antigen presented in a single HLA allele. Expanding this platform to a wider array of antigens and HLA alleles is a major opportunity although identifying scFvs with strong fidelity to the target pMHC can be challenging. Thus, these novel scFvs require rigorous testing for strict epitope and HLA specificities, as some scFv pMHC binders do show cross-reactivity with other HLA alleles.[58] In addition, CARs require high density expression of surface pMHC for cancer cell recognition and robust activity, and although IL-12 secretion by CAR T cells circumvents this issue, refinement of CAR architecture and signaling may also be necessary to improve efficacy.

Our scFv screening, validation, and testing pipeline not only accelerates the development of CAR T cell products targeting KRAS G12V but also holds potential for application across a wide range of neoantigens. This versatile regime enables the rapid identification and optimization of binders customized for diverse tumor-specific mutations, providing for a scalable approach to personalized medicine in solid tumors. As advances in AI-driven protein design become increasingly sophisticated, our workflow stands to benefit significantly from integrating targeted *in silico* predictions, enhancing the speed, precision, and resolution of scFv discovery. Future work could also explore combinatorial CAR-T therapies targeting multiple neoantigens within a single tumor, addressing tumor heterogeneity and reducing the likelihood of antigen escape. This approach holds promise for creating more comprehensive and durable treatments for solid tumors and beyond, including autoimmune diseases, infectious diseases, and chronic inflammatory conditions.

RESOURCE AVAILABILITY

Lead contact

Further information and requests for resources and reagents should be directed to and will be fulfilled by the lead contact, Daniel J. Powell Jr. (poda@pennmedicine.upenn.edu).

Materials availability

Plasmids and materials generated in this study will be made available on request, but we may require a payment and/or a completed materials transfer agreement if there is potential for commercial application.

Data and code availability

All data reported in this paper will be shared by the lead contact upon request. This paper does not report original code. Any additional information required to reanalyze the data reported in this paper is available from the lead contact upon request.

ACKNOWLEDGMENTS

The authors thank the University of Pennsylvania (UPenn) Stem Cell and Xenograft Core, Small Animal Imaging Facility, Human Immunology Core, and Flow

Cytometry Core for their technical support. We acknowledge Drs. Joseph Fraietta and Saar Gill for insights and feedback. We thank Song-My Hoang and Lumicks for providing z-Movi test equipment, experimental support, and analysis. Funding was provided in part by R01EB026892, R01CA260902 (D.J.P.) and SU2C/Lustgarten Foundation Pancreatic Cancer Collective, SUC-AACR-PCC-07-18 (B.M.C.). A.B. received funding from T32GM008076 and the Blavatnik Family Fellowship. J.L. was supported by a National Science Foundation Research Fellowship award, DGE-2236662. Graphics were created with BioRender and GraphPad Prism.

AUTHOR CONTRIBUTIONS

D.J.P. and P.M.S. conceived the study. D.J.P. designed and supervised the study. A.B. and J.L. designed experiments, conducted experiments and analyzed data. N.W. assisted in experimental design. A.L.G. and N.W. provided assistance in running experiments. M.U. and B.R.K. isolated and screened pMHC antibodies. M.A.P. managed and assisted with animal protocols. A.S.B., J.L., and B.M.C. generated cell lines used in assays. A.B., J.L., M. D.B., and D.J.P. wrote the manuscript. All authors reviewed, discussed and commented on results and the manuscript.

DECLARATION OF INTERESTS

D.J.P., A.B., and B.R.K. are co-inventors on provisional patent application 63/657,596 which incorporates discoveries and inventions described here. D.J.P. is a member of the scientific advisory boards for Crossbow Therapeutics, Bellicum Pharmaceuticals and InsTIL Bio. D.J.P. is inventor on patents and/or patent applications licensed to Prescient Therapeutics, Kite, and Miltenyi Biotec and receives license revenue from those licenses. B.R.K. and M.D.B. are co-founders of Myrio Tx. M.U., B.R.K., and M.D.B are current employees of Myrio Tx. P.M.S. is a former employee of Myrio Tx.

STAR★METHODS

Detailed methods are provided in the online version of this paper and include the following:

- KEY RESOURCES TABLE
- EXPERIMENTAL MODEL AND SUBJECT DETAILS
  - Cell lines and primary human T cells
  - Animal model details
- METHOD DETAILS
  - ReD platform screening for anti-mKRAS pMHC scFv
  - ScFv affinity measurements
  - Steady-state scFv binding assay
  - Bispecific T cell engager cytotoxicity assay
  - Design and molecular cloning of lentiviral constructs
  - Lentivirus production
  - Generation of mKRAS NeoCARs: T-Cell activation, transduction and expansion
  - Cancer cell lines maintenance, characterization, and transduction
  - TCR knockout in CAR-T cells using CRISPR/Cas9 RNPs
  - Flow cytometry
  - Peptide titration/pulsing
  - Luficerace based killing assays
  - Cell binding avidity assay
  - MHC I upregulation assay
  - Incucyte based spheroid assays
  - Stimulation based assays
  - Animal studies
- QUANTIFICATION AND STATISTICAL ANALYSIS

SUPPLEMENTAL INFORMATION

Supplemental information can be found online at https://doi.org/10.1016/j.ccell.2025.05.006.

Received: June 17, 2024
Revised: March 4, 2025
Accepted: May 15, 2025
Published: June 5, 2025

REFERENCES

1. Porter, D.L., Levine, B.L., Kalos, M., Bagg, A., and June, C.H. (2011). Chimeric antigen receptor-modified T cells in chronic lymphoid leukemia. N. Engl. J. Med. *365*, 725–733. https://doi.org/10.1056/NEJMoa1103849.
2. Kochenderfer, J.N., Wilson, W.H., Janik, J.E., Dudley, M.E., Stetler-Stevenson, M., Feldman, S.A., Maric, I., Raffeld, M., Nathan, D.A.N., Lanier, B.J., et al. (2010). Eradication of B-lineage cells and regression of lymphoma in a patient treated with autologous T cells genetically engineered to recognize CD19. Blood *116*, 4099–4102. https://doi.org/10.1182/blood-2010-04-281931.
3. Brentjens, R.J., Rivière, I., Park, J.H., Davila, M.L., Wang, X., Stefanski, J., Taylor, C., Yeh, R., Bartido, S., Borquez-Ojeda, O., et al. (2011). Safety and persistence of adoptively transferred autologous CD19-targeted T cells in patients with relapsed or chemotherapy refractory B-cell leukemias. Blood *118*, 4817–4828. https://doi.org/10.1182/blood-2011-04-348540.
4. Lee, D.W., Kochenderfer, J.N., Stetler-Stevenson, M., Cui, Y.K., Delbrook, C., Feldman, S.A., Fry, T.J., Orentas, R., Sabatino, M., Shah, N.N., et al. (2015). T cells expressing CD19 chimeric antigen receptors for acute lymphoblastic leukaemia in children and young adults: a phase 1 dose-escalation trial. Lancet *385*, 517–528. https://doi.org/10.1016/S0140-6736(14)61403-3.
5. van der Stegen, S.J.C., Hamieh, M., and Sadelain, M. (2015). The pharmacology of second-generation chimeric antigen receptors. Nat. Rev. Drug Discov. *14*, 499–509. https://doi.org/10.1038/nrd4597.
6. Anderson, K.G., Stromnes, I.M., and Greenberg, P.D. (2017). Obstacles Posed by the Tumor Microenvironment to T cell Activity: A Case for Synergistic Therapies. Cancer Cell *31*, 311–325. https://doi.org/10.1016/j.ccell.2017.02.008.
7. Beatty, G.L., and Moon, E.K. (2014). Chimeric antigen receptor T cells are vulnerable to immunosuppressive mechanisms present within the tumor microenvironment. OncoImmunology *3*, e970027. https://doi.org/10.4161/21624011.2014.970027.
8. Zhang, L., Morgan, R.A., Beane, J.D., Zheng, Z., Dudley, M.E., Kassim, S. H., Nahvi, A.V., Ngo, L.T., Sherry, R.M., Phan, G.Q., et al. (2015). Tumor-infiltrating lymphocytes genetically engineered with an inducible gene encoding interleukin-12 for the immunotherapy of metastatic melanoma. Clin. Cancer Res. *21*, 2278–2288. https://doi.org/10.1158/1078-0432.CCR-14-2085.
9. Hsu, C., Jones, S.A., Cohen, C.J., Zheng, Z., Kerstann, K., Zhou, J., Robbins, P.F., Peng, P.D., Shen, X., Gomes, T.J., et al. (2007). Cytokine-independent growth and clonal expansion of a primary human CD8+ T-cell clone following retroviral transduction with the IL-15 gene. Blood *109*, 5168–5177. https://doi.org/10.1182/blood-2006-06-029173.
10. Morgan, R.A., Yang, J.C., Kitano, M., Dudley, M.E., Laurencot, C.M., and Rosenberg, S.A. (2010). Case report of a serious adverse event following the administration of T cells transduced with a chimeric antigen receptor recognizing ERBB2. Mol. Ther. *18*, 843–851. https://doi.org/10.1038/mt.2010.24.
11. Haas, A.R., Golden, R.J., Litzky, L.A., Engels, B., Zhao, L., Xu, F., Taraszka, J.A., Ramones, M., Granda, B., Chang, W.J., et al. (2023). Two cases of severe pulmonary toxicity from highly active mesothelin-directed CAR T cells. Mol. Ther. *31*, 2309–2325. https://doi.org/10.1016/j.ymthe.2023.06.006.
12. Majzner, R.G., and Mackall, C.L. (2019). Clinical lessons learned from the first leg of the CAR T cell journey. Nat. Med. *25*, 1341–1355. https://doi.org/10.1038/s41591-019-0564-6.
13. Xu, X., Sun, Q., Liang, X., Chen, Z., Zhang, X., Zhou, X., Li, M., Tu, H., Liu, Y., Tu, S., and Li, Y. (2019). Mechanisms of Relapse After CD19 CAR T-Cell Therapy for Acute Lymphoblastic Leukemia and Its Prevention and

Treatment Strategies. Front. Immunol. *10*, 2664. https://doi.org/10.3389/fimmu.2019.02664.

14. Tsherniak, A., Vazquez, F., Montgomery, P.G., Weir, B.A., Kryukov, G., Cowley, G.S., Gill, S., Harrington, W.F., Pantel, S., Krill-Burger, J.M., et al. (2017). Defining a Cancer Dependency Map. Cell *170*, 564–576. https://doi.org/10.1016/j.cell.2017.06.010.
15. Arnaud, M., Coukos, G., and Harari, A. (2023). Towards next-generation TIL therapy: TILs enriched in neoepitope-specific T cells. Clin. Transl. Med. *13*, e1174. https://doi.org/10.1002/ctm2.1174.
16. Leko, V., and Rosenberg, S.A. (2020). Identifying and Targeting Human Tumor Antigens for T Cell-Based Immunotherapy of Solid Tumors. Cancer Cell *38*, 454–472. https://doi.org/10.1016/j.ccell.2020.07.013.
17. Bobisse, S., Genolet, R., Roberti, A., Tanyi, J.L., Racle, J., Stevenson, B.J., Iseli, C., Michel, A., Le Bitoux, M.A., Guillaume, P., et al. (2018). Sensitive and frequent identification of high avidity neo-epitope specific CD8 (+) T cells in immunotherapy-naive ovarian cancer. Nat. Commun. *9*, 1092. https://doi.org/10.1038/s41467-018-03301-0.
18. Lee, J.K., Sivakumar, S., Schrock, A.B., Madison, R., Fabrizio, D., Gjoerup, O., Ross, J.S., Frampton, G.M., Napalkov, P., Montesion, M., et al. (2022). Comprehensive pan-cancer genomic landscape of KRAS altered cancers and real-world outcomes in solid tumors. npj Precis. Oncol. *6*, 91. https://doi.org/10.1038/s41698-022-00334-z.
19. Choi, J., Goulding, S.P., Conn, B.P., McGann, C.D., Dietze, J.L., Kohler, J., Lenkala, D., Boudot, A., Rothenberg, D.A., Turcott, P.J., et al. (2021). Systematic discovery and validation of T cell targets directed against oncogenic KRAS mutations. Cell Rep. Methods *1*, 100084.
20. Wang, Q.J., Yu, Z., Griffith, K., Hanada, K.i., Restifo, N.P., and Yang, J.C. (2016). Identification of T-cell Receptors Targeting KRAS-Mutated Human Tumors. Cancer Immunol. Res. *4*, 204–214. https://doi.org/10.1158/2326-6066.CIR-15-0188.
21. Bear, A.S., Blanchard, T., Cesare, J., Ford, M.J., Richman, L.P., Xu, C., Baroja, M.L., McCuaig, S., Costeas, C., Gabunia, K., et al. (2021). Biochemical and functional characterization of mutant KRAS epitopes validates this oncoprotein for immunological targeting. Nat. Commun. *12*, 4365. https://doi.org/10.1038/s41467-021-24562-2.
22. Milone, M.C., Xu, J., Chen, S.J., Collins, M.A., Zhou, J., Powell, D.J., Jr., and Melenhorst, J.J. (2021). Engineering enhanced CAR T-cells for improved cancer therapy. Nat. Cancer *2*, 780–793. https://doi.org/10.1038/s43018-021-00241-5.
23. Kath, J., Du, W., Martini, S., Elsallab, M., Franke, C., Hartmann, L., Drosdek, V., Glaser, V., Stein, M., Schmueck-Henneresse, M., et al. (2023). CAR NK-92 cell-mediated depletion of residual TCR+ cells for ultrapure allogeneic TCR-deleted CAR T-cell products. Blood Adv. *7*, 4124–4134. https://doi.org/10.1182/bloodadvances.2022009397.
24. Walker, A.J., Majzner, R.G., Zhang, L., Wanhainen, K., Long, A.H., Nguyen, S.M., Lopomo, P., Vigny, M., Fry, T.J., Orentas, R.J., and Mackall, C.L. (2017). Tumor Antigen and Receptor Densities Regulate Efficacy of a Chimeric Antigen Receptor Targeting Anaplastic Lymphoma Kinase. Mol. Ther. *25*, 2189–2201. https://doi.org/10.1016/j.ymthe.2017.06.008.
25. Yeku, O.O., Purdon, T.J., Koneru, M., Spriggs, D., and Brentjens, R.J. (2017). Armored CAR T cells enhance antitumor efficacy and overcome the tumor microenvironment. Sci. Rep. *7*, 10541. https://doi.org/10.1038/s41598-017-10940-8.
26. Aspuria, P.J., Vivona, S., Bauer, M., Semana, M., Ratti, N., McCauley, S., Riener, R., de Waal Malefyt, R., Rokkam, D., Emmerich, J., et al. (2021). An orthogonal IL-2 and IL-2Rbeta system drives persistence and activation of CAR T cells and clearance of bulky lymphoma. Sci. Transl. Med. *13*, eabg7565. https://doi.org/10.1126/scitranslmed.abg7565.
27. Liu, Y., Di, S., Shi, B., Zhang, H., Wang, Y., Wu, X., Luo, H., Wang, H., Li, Z., and Jiang, H. (2019). Armored Inducible Expression of IL-12 Enhances Antitumor Activity of Glypican-3-Targeted Chimeric Antigen Receptor-Engineered T Cells in Hepatocellular Carcinoma. J. Immunol. *203*, 198–207. https://doi.org/10.4049/jimmunol.1800033.
28. Hu, B., Ren, J., Luo, Y., Keith, B., Young, R.M., Scholler, J., Zhao, Y., and June, C.H. (2017). Augmentation of Antitumor Immunity by Human and Mouse CAR T Cells Secreting IL-18. Cell Rep. *20*, 3025–3033. https://doi.org/10.1016/j.celrep.2017.09.002.
29. Kunert, A., Chmielewski, M., Wijers, R., Berrevoets, C., Abken, H., and Debets, R. (2017). Intra-tumoral production of IL18, but not IL12, by TCR-engineered T cells is non-toxic and counteracts immune evasion of solid tumors. OncoImmunology *7*, e1378842. https://doi.org/10.1080/2162402X.2017.1378842.
30. Smole, A., Benton, A., Poussin, M.A., Eiva, M.A., Mezzanotte, C., Camisa, B., Greco, B., Sharma, P., Minutolo, N.G., Gray, F., et al. (2022). Expression of inducible factors reprograms CAR-T cells for enhanced function and safety. Cancer Cell *40*, 1470–1487. https://doi.org/10.1016/j.ccell.2022.11.006.
31. Beasley, M.D., Niven, K.P., Winnall, W.R., and Kiefel, B.R. (2015). Bacterial cytoplasmic display platform Retained Display (ReD) identifies stable human germline antibody frameworks. Biotechnol. J. *10*, 783–789. https://doi.org/10.1002/biot.201400560.
32. Yarmarkovich, M., Marshall, Q.F., Warrington, J.M., Premaratne, R., Farrel, A., Groff, D., Li, W., di Marco, M., Runbeck, E., Truong, H., et al. (2023). Targeting of intracellular oncoproteins with peptide-centric CARs. Nature *623*, 820–827. https://doi.org/10.1038/s41586-023-06706-0.
33. Eichmann, M., de Ru, A., van Veelen, P.A., Peakman, M., and Kronenberg-Versteeg, D. (2014). Identification and characterisation of peptide binding motifs of six autoimmune disease-associated human leukocyte antigen-class I molecules including HLA-B*39:06. Tissue Antigens *84*, 378–388. https://doi.org/10.1111/tan.12413.
34. Jaravine, V., Mösch, A., Raffegerst, S., Schendel, D.J., and Frishman, D. (2017). Expitope 2.0: a tool to assess immunotherapeutic antigens for their potential cross-reactivity against naturally expressed proteins in human tissues. BMC Cancer *17*, 892. https://doi.org/10.1186/s12885-017-3854-8.
35. Zhu, Z., and Carter, P. (1995). Identification of heavy chain residues in a humanized anti-CD3 antibody important for efficient antigen binding and T cell activation. J. Immunol. *155*, 1903–1910.
36. Carpenito, C., Milone, M.C., Hassan, R., Simonet, J.C., Lakhal, M., Suhoski, M.M., Varela-Rohena, A., Haines, K.M., Heitjan, D.F., Albelda, S.M., et al. (2009). Control of large, established tumor xenografts with genetically retargeted human T cells containing CD28 and CD137 domains. Proc. Natl. Acad. Sci. USA *106*, 3360–3365. https://doi.org/10.1073/pnas.0813101106.
37. Batard, P., Peterson, D.A., Devêvre, E., Guillaume, P., Cerottini, J.C., Rimoldi, D., Speiser, D.E., Winther, L., and Romero, P. (2006). Dextramers: new generation of fluorescent MHC class I/peptide multimers for visualization of antigen-specific CD8+ T cells. J. Immunol. Methods *310*, 136–148. https://doi.org/10.1016/j.jim.2006.01.006.
38. Leonard, J.P., Sherman, M.L., Fisher, G.L., Buchanan, L.J., Larsen, G., Atkins, M.B., Sosman, J.A., Dutcher, J.P., Vogelzang, N.J., and Ryan, J.L. (1997). Effects of single-dose interleukin-12 exposure on interleukin-12-associated toxicity and interferon-gamma production. Blood *90*, 2541–2548.
39. Scott, P. (1993). IL-12: initiation cytokine for cell-mediated immunity. Science *260*, 496–497. https://doi.org/10.1126/science.8097337.
40. Zhang, S., Kohli, K., Black, R.G., Yao, L., Spadinger, S.M., He, Q., Pillarisetty, V.G., Cranmer, L.D., Van Tine, B.A., Yee, C., et al. (2019). Systemic Interferon-gamma Increases MHC Class I Expression and T-cell Infiltration in Cold Tumors: Results of a Phase 0 Clinical Trial. Cancer Immunol. Res. *7*, 1237–1243. https://doi.org/10.1158/2326-6066.CIR-18-0940.
41. Chong, C., Marino, F., Pak, H., Racle, J., Daniel, R.T., Müller, M., Gfeller, D., Coukos, G., and Bassani-Sternberg, M. (2018). High-throughput and Sensitive Immunopeptidomics Platform Reveals Profound Interferongamma-Mediated Remodeling of the Human Leukocyte Antigen (HLA) Ligandome. Mol. Cell. Proteomics *17*, 533–548. https://doi.org/10.1074/mcp.TIR117.000383.
42. Komov, L., Kadosh, D.M., Barnea, E., Milner, E., Hendler, A., and Admon, A. (2018). Cell Surface MHC Class I Expression Is Limited by the

Availability of Peptide-Receptive "Empty" Molecules Rather than by the Supply of Peptide Ligands. Proteomics *18*, e1700248. https://doi.org/10.1002/pmic.201700248.

43. Kulkarni, S., Ramsuran, V., Rucevic, M., Singh, S., Lied, A., Kulkarni, V., O'HUigin, C., Le Gall, S., and Carrington, M. (2017). Posttranscriptional Regulation of HLA-A Protein Expression by Alternative Polyadenylation Signals Involving the RNA-Binding Protein Syncrip. J. Immunol. *199*, 3892–3899. https://doi.org/10.4049/jimmunol.1700697.
44. Shafer, P., Kelly, L.M., and Hoyos, V. (2022). Cancer Therapy With TCR-Engineered T Cells: Current Strategies, Challenges, and Prospects. Front. Immunol. *13*, 835762. https://doi.org/10.3389/fimmu.2022.835762.
45. Lowe, K.L., Cole, D., Kenefeck, R., OKelly, I., Lepore, M., and Jakobsen, B. K. (2019). Novel TCR-based biologics: mobilising T cells to warm 'cold' tumours. Cancer Treat Rev. *77*, 35–43. https://doi.org/10.1016/j.ctrv.2019.06.001.
46. Tokatlian, T., Asuelime, G.E., Naradikian, M.S., Mock, J.Y., Daris, M.E., Martin, A.D., Toledo Warshaviak, D., Kamb, A., and Hamburger, A.E. (2022). Chimeric Antigen Receptors Directed at Mutant KRAS Exhibit an Inverse Relationship Between Functional Potency and Neoantigen Selectivity. Cancer Res. Commun. *2*, 58–65. https://doi.org/10.1158/2767-9764.CRC-21-0165.
47. Majzner, R.G., and Mackall, C.L. (2018). Tumor Antigen Escape from CAR T-cell Therapy. Cancer Discov. *8*, 1219–1226. https://doi.org/10.1158/2159-8290.CD-18-0442.
48. Jia, Z., Ragoonanan, D., Mahadeo, K.M., Gill, J., Gorlick, R., Shpal, E., and Li, S. (2022). IL12 immune therapy clinical trial review: Novel strategies for avoiding CRS-associated cytokines. Front. Immunol. *13*, 952231. https://doi.org/10.3389/fimmu.2022.952231.
49. Sun, L., He, C., Nair, L., Yeung, J., and Egwuagu, C.E. (2015). Interleukin 12 (IL-12) family cytokines: Role in immune pathogenesis and treatment of CNS autoimmune disease. Cytokine *75*, 249–255. https://doi.org/10.1016/j.cyto.2015.01.030.
50. Wang, P., Li, X., Wang, J., Gao, D., Li, Y., Li, H., Chu, Y., Zhang, Z., Liu, H., Jiang, G., et al. (2017). Re-designing Interleukin-12 to enhance its safety and potential as an anti-tumor immunotherapeutic agent. Nat. Commun. *8*, 1395. https://doi.org/10.1038/s41467-017-01385-8.
51. Lee, E.H.J., Murad, J.P., Christian, L., Gibson, J., Yamaguchi, Y., Cullen, C., Gumber, D., Park, A.K., Young, C., Monroy, I., et al. (2023). Antigen-dependent IL-12 signaling in CAR T cells promotes regional to systemic disease targeting. Nat. Commun. *14*, 4737. https://doi.org/10.1038/s41467-023-40115-1.
52. Spiegel, J.Y., Patel, S., Muffly, L., Hossain, N.M., Oak, J., Baird, J.H., Frank, M.J., Shiraz, P., Sahaf, B., Craig, J., et al. (2021). CAR T cells with dual targeting of CD19 and CD22 in adult patients with recurrent or refractory B cell malignancies: a phase 1 trial. Nat. Med. *27*, 1419–1431. https://doi.org/10.1038/s41591-021-01436-0.
53. Chockley, P.J., Ibanez-Vega, J., Krenciute, G., Talbot, L.J., and Gottschalk, S. (2023). Synapse-tuned CARs enhance immune cell anti-tumor activity. Nat. Biotechnol. *41*, 1434–1445. https://doi.org/10.1038/s41587-022-01650-2.
54. Mansilla-Soto, J., Eyquem, J., Haubner, S., Hamieh, M., Feucht, J., Paillon, N., Zucchetti, A.E., Li, Z., Sjöstrand, M., Lindenbergh, P.L., et al. (2022). HLA-independent T cell receptors for targeting tumors with low antigen density. Nat. Med. *28*, 345–352. https://doi.org/10.1038/s41591-021-01621-1.
55. Baeuerle, P.A., Ding, J., Patel, E., Thorausch, N., Horton, H., Gierut, J., Scarfo, I., Choudhary, R., Kiner, O., Krishnamurthy, J., et al. (2019). Synthetic TRuC receptors engaging the complete T cell receptor for potent anti-tumor response. Nat. Commun. *10*, 2087. https://doi.org/10.1038/s41467-019-10097-0.
56. Wang, S.S., Luong, K., Gracey, F.M., Jabar, S., McColl, B., Cross, R.S., and Jenkins, M.R. (2021). A Novel Peptide-MHC Targeted Chimeric Antigen Receptor T Cell Forms a T Cell-like Immune Synapse. Biomedicines *9*, 1875. https://doi.org/10.3390/biomedicines9121875.
57. Davenport, A.J., Cross, R.S., Watson, K.A., Liao, Y., Shi, W., Prince, H.M., Beavis, P.A., Trapani, J.A., Kershaw, M.H., Ritchie, D.S., et al. (2018). Chimeric antigen receptor T cells form nonclassical and potent immune synapses driving rapid cytotoxicity. Proc. Natl. Acad. Sci. USA *115*, E2068–E2076. https://doi.org/10.1073/pnas.1716266115.
58. Sun, Y., Florio, T.J., Gupta, S., Young, M.C., Marshall, Q.F., Garfinkle, S.E., Papadaki, G.F., Truong, H.V., Mycek, E., Li, P., et al. (2023). Structural principles of peptide-centric chimeric antigen receptor recognition guide therapeutic expansion. Sci. Immunol. *8*, eadj5792. https://doi.org/10.1126/sciimmunol.adj5792.
59. Posey, A.D., Jr., Schwab, R.D., Boesteanu, A.C., Steentoft, C., Mandel, U., Engels, B., Stone, J.D., Madsen, T.D., Schreiber, K., Haines, K.M., et al. (2016). Engineered CAR T Cells Targeting the Cancer-Associated Tn-Glycoform of the Membrane Mucin MUC1 Control Adenocarcinoma. Immunity (Camb., Mass.) *44*, 1444–1454. https://doi.org/10.1016/j.immuni.2016.05.014.

Please cite this article in press as: Benton et al., Mutant KRAS peptide targeted CAR-T cells engineered for cancer therapy, Cancer Cell (2025), https://doi.org/10.1016/j.ccell.2025.05.006

STAR★METHODS

KEY RESOURCES TABLE

REAGENT or RESOURCE	SOURCE	IDENTIFIER
Antibodies		
MHC I Dextramers-PE	Immudex	NA
Lightning Link APC	R&D systems	Cat# 705-0005
Goat polyclonal anti-human IgG	Sigma-Aldrich	Cat# I1886-2ML; RRID: AB_260125
CD8 BV786	BD Biosciences	Cat# 563823; RRID: AB_2687487
CD4 Fitc	Biolegend	Cat# 317407; RRID: AB_571950
CD3 Biotin	BioLegend	Cat# 300404; RRID: AB_314058
CD3 PerCPCy5.5	Biolegend	Cat# 344808; RRID: AB_10640736
Live/Dead Aqua	Thermo-Fischer Scientific	Cat# L-34966
HLA-A,B,C PE	BD Biosciences	Cat# 555553; RRID: AB_395936
HLA-A*11:01 Biotin	USBiological	Cat# H6098-28A
Streptavidin PE	BD Biosciences	Cat# 349023; RRID: AB_2868860
CD45 PE	BioLegend	Cat# 304008; RRID: AB_314396
Biological samples		
Primary T cells	UPenn Human Immunology Core.	NA
Chemicals, peptides, and recombinant proteins		
anti-CD3/CD28 dynabeads	Invitrogen	Cat# 402.03D
Streptavidin C1 Dynabeads	Invitrogen	Cat# 65001
n-Octyl-β-D-Thioglucopyranoside	Anatrace	Cat# 85618-21-9
Nickel NTA Agarose Resin	ABT	Cat# 6BCL-NTANi-X
anti-biotin microbeads	Miltenyi	Cat# 130-105-637
PMA+ionomycin	eBioscience	Cat# 00-4970-93
RPMI 1640	GIBCO	Cat# 72400-047
Foetal bovine serum (FBS)	VWR	Cat# S170G
KRAS 10-mer Peptides	Genscript	NA
Critical commercial assays		
Amaxa P3 Primary Cell kit and protocol	Lonza	Cat# V4XP-3012
Experimental models: Cell lines		
HEK 293T	ATCC	Cat# CRL-3216; RRID: CVCL_0063
Jurkat E6.1	ATCC	Cat# TIB-152; RRID: CVCL_0367
COR-L23	ECACC	Cat# 92031919; RRID: CVCL_1139
COR-L23 HLA-A*11:01	University of Pennsylvania, Dr. Beatriz M. Carreno	NA
YAPC	DSMZ	Cat# ACC 382; RRID: CVCL_1794
YAPC HLA-A*11:01	University of Pennsylvania, Dr. Beatriz M. Carreno	NA
K562 HLA-A*2:01	University of Pennsylvania, Dr. Beatriz M. Carreno	NA
K562 HLA-A*11:01	University of Pennsylvania, Dr. Beatriz M. Carreno	NA
XL1-Blue Supercompetent Cells	Agilent Technologies	Cat# 200236
Experimental models: Organisms/strains		
NOD/scid/IL2rg	University of Pennsylvania Stem Cell and Xenograft Core	RRID:IMSR_JAX:005557

(*Continued on next page*)

Please cite this article in press as: Benton et al., Mutant KRAS peptide targeted CAR-T cells engineered for cancer therapy, Cancer Cell (2025), https://doi.org/10.1016/j.ccell.2025.05.006

Continued

REAGENT or RESOURCE	SOURCE	IDENTIFIER
Recombinant DNA		
Lentiviral constructs	This manuscript	NA
Software and algorithms		
GraphPad Prism	GraphPad Software	https://www.graphpad.com/
FlowJo	BD	https://www.flowjo.com/
bioRender	bioRender	https://www.biorender.com/
ScanProsite	Expasy	https://www.prosite.expasy.org/

EXPERIMENTAL MODEL AND SUBJECT DETAILS

Cell lines and primary human T cells

All cell lines were cultured in complete medium (CM) comprising of RPMI 1640 (GIBCO) supplemented with 10% FBS (VWR), 100 U/mL of penicillin, and 100 μg/mL of streptomycin at 37°C and 5% CO_2. Cell line origins are listed in the Key Resource Table. All cell lines were routinely tested for mycoplasma. Human CAR-T cells were generated from normal donor T cells provided by the University of Pennsylvania Human Immunology Core. All primary T cell studies were covered through approval by the University of Pennsylvania Institutional Review Board (IRB). All de-identified donors signed approved consent forms. Details are listed in method details (Cell lines section). Normal donor T cells: T cells were isolated from healthy volunteers who previously signed an informed consent, which authorized use for general research purposes. Samples were centrally collected and sent to the laboratory for processing after complete anonymization. Normal donor T cells were cultured in CM with cytokine supplementation (Biolegend).

Animal model details

NOD/SCID/IL2rγ^{null} (NSG) mice were purchased from the Stem Cell and Xenograft Core (University of Pennsylvania). Mice (6−12 weeks old) were kept in a pathogen-free environment within individually ventilated cages. Animal studies were performed in full accordance with the University of Pennsylvania Institutional Animal Care and Use Committee (IACUC protocol n. 805773). The specific designs of *in vivo* studies are indicated for each experiment in the manuscript. Both male and female animals were employed for separate experimental replicates.

METHOD DETAILS

ReD platform screening for anti-mKRAS pMHC scFv

HLA-A*11:01 MHC complexes for antibody discovery and all characterization assays were expressed in *E. coli* as insoluble inclusion bodies and were refolded via dialysis against glutathione buffer with mKRAS peptides as per standard methods. Myrio's Ruby scFv library (>10^{11} clone diversity) was panned for two rounds using mKRAS peptide-MHC bound to MyOne Streptavidin C1 Dynabeads (ThermoFisher). Panned library output were transferred into the Retained Display (ReD) cell-display platform (Myrio Bio) and cells were permeabilized using 0.5% n-octyl β-d-thioglucopyranoside (Anatrace) and labeled using mKRAS MHC ligated to fluorophores excitable by 405 nm and 488 nm lasers. Cells that were positive for target binding were isolated using the FACSMelody sorter (Becton-Dickinson).

After two rounds of positive selection, two further FACS rounds were conducted using counter-labelled WT KRAS MHC complexed with unrelated peptides. After 4 rounds of FACS, individual colonies were picked and grown in 96-well plates before scFv induction, cell permeabilization, and mKRAS MHC labelling and detection by CytoFLEX (Beckman Coulter).

Clones that were identified as binding specifically to the target complex were sequenced and unique scFvs were expressed as fusions to the AviTag biotinylation motif in *E. coli*. Biotinylated scFv protein was released via permeabilization with 0.5% n-octyl β-d-thioglucopyranoside and purified to ~90% purity on Nickel NTA agarose resin (ABT).

ScFv affinity measurements

Affinity measurements were performed using the Gator Bio biolayer interferometry instrument (Gator Bio) and analyzed using GatorOne software. Streptavidin biosensors were loaded with AviTag-biotinylated scFv, blocked with biotin, washed in PBS, and then associated with mKRAS MHC protein in PBS.

Steady-state scFv binding assay

A bead-based fluorometric assay was developed to measure scFv binding to soluble MHC complex. Briefly, 50 μg streptavidin-coated Dynabeads were incubated with excess biotinylated scFv before being blocked with free biotin and washed in PBS. Fluorophore-labelled MHC complex was added to a concentration of 3.5 nM and incubated for 1 hour at 4°C, followed by 10 minutes at

Please cite this article in press as: Benton et al., Mutant KRAS peptide targeted CAR-T cells engineered for cancer therapy, Cancer Cell (2025), https://doi.org/10.1016/j.ccell.2025.05.006

25°C. Binding of MHC by scFv-coated beads was quantified using the CytoFLEX instrument and normalised to controls, including binding by beads without scFv and binding to unrelated MHC complex.

The bead-based assay described above was used to assess scFv binding to a panel of 95 unrelated peptides refolded in the relevant HLA compared to target pHLA, as a preliminary readout of scFv selectivity. It was also used to characterize the 'footprint' of scFv binding on target peptide-HLA using X-scanning mutagenesis for the assessment of scFv cross-reactivity toward peptides with homology to target peptide, identified using sequence-based analyses. Binding motifs determined by X-Scanning were uploaded to ScanProsite (prosite.expasy.org) to analyze them against protein sequence databases (e.g. UniProtKB/Swiss-Prot) and identify any known human proteins containing the tolerated amino acids in the correct sequence. Identified peptides were then cross-referenced with The Immune Epitope Database (IEDB.org) to determine whether any are known to be presented.

Bispecific T cell engager cytotoxicity assay

Monoallelic cell lines stably expressing single chain B2m-HLA-A*11:01 fusion proteins in addition to a ICP47 HSV TAP inhibitor and eGFP were established using the K562 cell line (ATCC), which lacks surface expression of HLA-A alleles.

For bispecific-mediated cytotoxicity assays, K562 target cells expressing the HLA allele of interest were washed and resuspended in fresh CM containing KRAS G12V or wildtype (7-16) peptide at 1uM concentration or solvent control (DMSO). The cell-peptide suspensions were then aliquoted into 96 well plates at 15,000 cells per well and incubated for 3 hours at 28°C and 5% CO_2. Bispecific antibodies to be tested were added to the peptide-pulsed cells and incubated for a further 30 minutes at 28°C, before addition of CD3/CD28-activated human cytotoxic T lymphocytes (50,000 per well; effector:target ratio of 3:1). Assays were then incubated for 24 hours at 37°C and 5% CO_2, and flow cytometry used to measure live and intact target cells on the basis of Sytox Blue viability staining and eGFP expression to discriminate target cells from effectors. Cytotoxicity was calculated relative to controls lacking bispecific antibodies. All measurements were carried out in triplicate.

Design and molecular cloning of lentiviral constructs

The lentiviral constructs designed and used in this study are listed in Table S1. The mKRAS scFv sequence was synthesized (Genscript) and cloned into 3rd generation self-inactivating (SIN) lentiviral transfer vector pTRPE[59] that The University of Pennsylvania uses for clinical CAR-T cell manufacturing. UniVect construct pASP18 was previously described by our group,[30] and construct pABL2 was generated by sub-cloning the RU96-14 CAR scFv into pASP19. All genetic constructs were prepared using standard digest and ligate restriction enzymes-based molecular cloning techniques and were sequence verified. All cloning and plasmid propagation steps were performed in XL1-Blue Supercompetent Cells (Agilent Technologies, Cat# 200236) to maintain integrity of lentiviral transfer plasmids.

Lentivirus production

The human embryonic kidney (HEK) 293 T cell line (ATCC) were grown to 70% confluency in CM at 37°C and 5% CO_2. UniVect transfer plasmid and lentiviral packaging plasmids pRSV.REV (Rev expression vector), pMDLg/p.RRE (Gag/Pol expression plasmid) and pVSV-G (VSV glycoprotein expression vector) were added to Opti-MEM (Thermo Cat. 31985088) at a 15:18:18:7 mass-unit ratio. This mixture was added to a 10:1 Opti-MEM and Lipofectamine 2000 (Thermo Cat# 11668019) mixture at 1:1 volume ratio and let incubate at RT for 15 min before addition to HEK 293T cells in fresh culturing media. Supernatants containing the lentivirus were collected at 24 h and 48 h and passed through 0.45 μm filters. Filtered lentivirus product was concentrated by ultracentrifugation at 25 000 rpm for 2.5 h and stored at -80°C. The viral titer was determined by transducing HEK 293T cells and expressed as Infection Units per mL.

Generation of mKRAS NeoCARs: T-Cell activation, transduction and expansion

Healthy donor primary human T cells were purchased from the Human Immunology Core (University of Pennsylvania). $CD4^+$ and $CD8^+$ T cells were combined at 1:1 ratio and stimulated with anti-CD3/CD28 dynabeads (Invitrogen) in a 3:1 ratio on Day 0. After 24 h (Day 1), lentivirus was added at a multiplicity of infection (MOI) of 1-5 (depending on the experiment). CM volume was doubled every 2 days until Day 6 when Dynabeads were removed by magnetic separation. Cells were then counted every 1-2 days by Coulter Counter (Beckman Coulter) and maintained at 0.75×10^6 cells/mL by addition of fresh IL-7/15 (10 ng/mL each, R&D systems) supplemented CM until day 11 when media was switched to non-supplemented CM. Cells were either frozen or used experimentally once the cell volume reached 280-330 fL at around Day 14. During manufacturing, T cells were maintained at 37°C and 5% CO_2. The transduction efficiency was determined by flow cytometry for the expression of relevant gene (mCherry or immune receptor). For experiments with Jurkat cell line, cells were transduced lentiviruses at various MOI 3 and used in experiments 3-5 days later.

Cancer cell lines maintenance, characterization, and transduction

The human cancer cell lines YAPC (KRASG12V), COR-L23 (KRASG12V), SW-620 (KRASG12V), BxPC-3 (KRASWT), CAKi-2 (HLA-A*11:01), PANC-1 (HLA-A*11:01, KRASG12D), and HCC-827 (HLA-A*11:01, KRASWT) were obtained from American Type Culture Collection (ATCC) and cultured according to protocols of the vendor. HLA-A*11:01 surface expression characterized with flow cytometry with antibody staining (USBiological). CAKi-2, PANC-1, and HCC-827 were transduced with a KRAS tandem minigene construct and purified as we previously reported.[21]

Please cite this article in press as: Benton et al., Mutant KRAS peptide targeted CAR-T cells engineered for cancer therapy, Cancer Cell (2025), https://doi.org/10.1016/j.ccell.2025.05.006

TCR knockout in CAR-T cells using CRISPR/Cas9 RNPs

Healthy donor primary human T cells were purchased from the Human Immunology Core (University of Pennsylvania). $CD4^+$ and $CD8^+$ T cells were combined at 1:1 number ratio. On Day 0 T-cells were centrifuged and resuspended in fresh CM supplemented with IL-2 (200 IU/μL, BioLegend) IL-7 and IL-15 (5 ng/mL each, R&D Systems) with a 1:1 ratio of CD3/28 Dynabeads. On Day 2 T-cells were debeaded and washed with PBS. 1μg TRAC targeting sgRNA (IDT) (5′-TGTGCTAGACATGAGGTCTA-3′) and 1μg SpyFi Cas9 (Aldevron) were added for 10 min. PBS was aspirated from washed T-cells and the 50e6/ml (1e6 in 20uL) cells were electroporated using the Amaxa P3 Primary Cell kit and protocol (Lonza) with a Lonza 4-D Nucleofector electroporation device (Cat# AAF-1002B model). After electroporation, cells were resuspended in IL-2 (200 IU/μL) IL-7 and IL-15 (5 ng/mL each) supplemented CM for ~12 days of additional expansion. On day 7 of expansion, edited TCR^- CAR-T cell products were purified by negative selection with anti-biotin microbeads (Miltenyi Cat# 130-105-637) and biotin conjugated anti-CD3 (Biolegend, Cat# 317320) on a MACS separation column (Miltenyi, Cat# 130-042-201) where the remaining CD3 positive, and therefore TCR^+, cells were removed. Flow through containing TCR^- cells was collected and cells were placed in fresh CM with cytokines.

Flow cytometry

Samples were spun down at 1300 RPM, then washed once with staining buffer. Samples collected from mice had 2 mL of ACK Lysis buffer added for 5 min to lyse red blood cells then washed once with PBS. Samples were stained for CAR surface expression for 30 minutes at room temperature with 100 μL solution containing the goat polyclonal anti-human IgG (Sigma-Aldrich, Cat# I1886-2ML) conjugated with Lightning-Link APC (Expedeon). After CAR staining, samples were washed three times with staining buffer and then incubated at 4°C for 30 minutes in 100 μL of an antibody cocktail to label the experimentally indicated human surface markers. Samples were washed three times and incubated with Live/Dead Aqua (Thermo-Fischer Scientific Cat# L-34966) for 10 minutes to discriminate live and dead cells. Samples were washed twice to remove Live/Dead Aqua before being run on a Fortessa.

Peptide titration/pulsing

K562 cells transduced with the indicated HLA-A construct were added to a 96 well plate at 20,000 cells/well in CM. For Jurkat based screens the following 10-mer KRAS peptides (A11 Mut: VVVGAVGVGK, A11 WT: VVVGAGGVGK, A2 Mut: KLVVVGAVGV, A2 WT: KLVVVGAGGV) were added to achieve a concentration of 1uM. For titrations, the indicated peptide and concentration was achieved for each replicate. After 90 min incubation at 37 C the peptide pulsed cells were centrifuged, washed with CM, then fresh CM was added. Next, mKRAS NeoCAR transduced Jurkat or primary T cells were normalized for transduction added to achieve an E:T ratio of 2:1 in 200μL CM. Target and Effector cells co-cultured for 24 h at 37°C and 5% CO_2 and supernatants were collected for cytokine quantification by ELISA according to the manufacturer's instructions (BioLegend) as follows: human hIFN-γ was detected by hIFN-γ (BioLegend, Cat# 430104), human hIL-2 was detected by hIL-2 (BioLegend, Cat# 431804) and hIL-12 was hIL-12 (BioLegend, Cat# 431704)

Luficerace based killing assays

Lytic function of mKRAS NeoCARs was measured using the LucScreen Extended-Glow Luciferase Reporter Gene Assay System (Applied Biosystems). NeoCAR-T cells and tumor cells expressing click beetle green luciferase (CBG) were combined at the indicated E:T ratios in a total of 200 μL CM in an white opaque walled flat bottom plate and co-cultured for 48 h at 37°C and 5% CO_2. Plates were centrifuged and 100 μL of medium was removed from each well for further analysis by ELISA. Luciferase buffer was added directly into the plate according to the manufacturer's protocol. Luciferase readings were obtained using a microplate reader (BioTek Synergy H4). Cytotoxicity was calculated using the following equation where: (1 - $luminescence_{(CAR\text{-}T\ cells\ +\ target\ cells)}$/$luminescence_{(Target\ cells)}$) x 100.

Cell binding avidity assay

COR-L tumor cells were attached in a monolayer on poly-L-lysine-coated chips for at least 3 h prior to testing on the z-Movi Cell Avidity Analyzer (Lumicks). CellTrace far-red labelled (ThermoFisher Scientific) CAR T cells from various donors were normalized for transduction efficiency and bound for 5 min prior to ramping up acoustic force from 0-1000 pN. Experiments were performed in triplicate with each of the three T cell conditions ran once on each chip. Cell detachment was analyzed using Ocean software. Experiments and analysis were conducted according to manufacturer recommendations.

MHC I upregulation assay

On Day 0 50,000 indicated target cells were added to a 24 well flat bottom plate. Next, mKRAS NeoCAR-T cells were normalized for transduction and added to achieve an E:T ratio of 2:1 in 1 mL CM. Target and effector cells co-cultured for 24 h at 37°C and 5% CO_2. On Day 1, fresh target cells were added to a new 24 well plate in 500μL. Co-cultures were centrifuged and 500μL of supernatant was added to the fresh target cells to achieve a final volume of 1 mL. Target cells were cultured with supernatants for 24 h. Additional supernatant was saved for cytokine quantification by ELISA. On Day 2 Target cells were detached form the plate with TrypLE express (ThermoFisher) and analyzed for MHC I expression by flow cytometry.

Please cite this article in press as: Benton et al., Mutant KRAS peptide targeted CAR-T cells engineered for cancer therapy, Cancer Cell (2025), https://doi.org/10.1016/j.ccell.2025.05.006

Incucyte based spheroid assays

On day -3 1,250 target cells expressing GFP were plated in a 96 well round bottom ultra-low attachment plate (S-bio) in 100μL CM. Next, mKRAS NeoCAR-T cells were normalized for transduction and 20,000 CAR+ cells were added to achieve an estimated E:T ratio of 2:1 in 200 μL CM. Additionally, 0.1 ug of CD45-PE was added to each well to visualize T cells. Co-cultures were placed in an Incucyte SX5 device (Sartorius) for 48 h and imaged every 3-6 hours in the trans, orange, and green channels. Normalized percent killing was calculated using fluorescence in the green channel and the equation (total intensity time=n / total intensity time=0) x 100.

Stimulation based assays

T cell products were stimulated according to specific experiment for 24 h either with 0.5x cell stimulation cocktail (Invitrogen), 1:1 CD3/28 beads, or through 2:1 E:T co-culture with COR-L target cells. Cytokine levels were measured by a sandwich ELISA according to the manufacturer's instructions (BioLegend) as follows: human hIFN-γ was detected by hIFN-γ (BioLegend, Cat# 430104), human hIL-2 was detected by hIL-2 (BioLegend, Cat# 431804) and hIL-12 was hIL-12 (BioLegend, Cat# 431704).

Animal studies

NOD/SCID/IL2rγ^{null} (NSG) mice were purchased from the Stem Cell and Xenograft Core (University of Pennsylvania). Female and male mice (6−12 weeks old) were kept in a pathogen-free environment within individually ventilated cages following protocols approved by the University of Pennsylvania Institutional Animal Care and Use Committee (IACUC protocol n. 805773). The specific designs of *in vivo* studies are indicated for each experiment in the manuscript. For human tumor models, mice were intravenously (i.v.) injected via tail veins with 0.25e6 COR-L23 A*11:01, CAKi-2-G12V, or YAPC-A11 tumor cells. After 7 days when tumors were established and confirmed by imaging, mKRAS NeoCARs were injected i.v. at doses indicated in the specific experiments in the figure. Tumor progression/clearance was measured via bioluminescence imaging and quantified as the total flux per second. Mice were sacrificed upon losing 20% body weight or reaching a total flux of more than 5e10 photons/s. Blood samples were collected via retro-orbital bleeds of days 18 and 25 post tumor injection. Number of peripheral blood T cells was quantified using countbright beads (Invitrogen). The staining panel consisted of anti-human CD3, anti-human CD45, anti-human CD8 and anti-human CD4. Plasma samples were collected from remaining blood and use for cytokine quantification by ELISA.

QUANTIFICATION AND STATISTICAL ANALYSIS

Information on specific statistical tests used is provided in the figure legends and/or Method Details. Statistical analysis was performed in GraphPad Prism 8.0 (GraphPad). Each figure legend denotes the statistical test used. All central tendencies indicate the mean, and all error bars indicate standard deviation unless otherwise indicated. Statistical analysis and tests performed included 2-tailed Student t test, Two-way ANOVA or ANOVA multiple-comparison with P values generated using Tukey's or Welch multiple-comparisons test. For non-parametric comparisons, we used Kruskal-Wallis tests. All t-tests were two-sided. In figures, p values are shown. Log-Rank Mantel-Cox test was used for survival analysis. Technical replicates were assumed to be normally distributed, otherwise no assumptions of normality were made. Statistical details of all experiments can be found in figure legends.